Check for updates

Received: 14 July 2023 | Revised: 1 September 2023 | Accepted: 4 September 2023

DOI: 10.1002/ardp.202300382

ARCH PHARM DPhG
Archiv der Pharmazie

FULL PAPER

Molecular docking, synthesis, anticancer activity, and metabolomics study of boronic acid ester-containing fingolimod derivatives

Doğukan Doyduk[1] | Burak Derkus[2] | Buse Sari[2] | Cemil Can Eylem[3] | Emirhan Nemutlu[3,4] | Yılmaz Yıldırır[1]

[1]Department of Chemistry, Faculty of Science, Gazi University, Ankara, Turkey

[2]Stem Cell Research Lab, Department of Chemistry, Faculty of Science, Ankara University, Ankara, Turkey

[3]Analytical Chemistry Division, Faculty of Pharmacy, Hacettepe University, Ankara, Turkey

[4]Bioanalytic and Omics Laboratory, Faculty of Pharmacy, Hacettepe University, Ankara, Turkey

Correspondence
Yılmaz Yıldırır, Department of Chemistry, Faculty of Science, Gazi University, Ankara 06560, Turkey.
Email: yildirir@gazi.edu.tr

Funding information
Gazi University Scientific Research Projects Unit, Grant/Award Number: 05/2020-25

Abstract

In recent years, drugs that contain boronic acid groups, such as ixazomib (Ninlaro™) and bortezomib (Velcade™), have been used in the treatment of bone marrow cancer. The activity of compounds has been found to increase with the addition of boron atoms to the structure. In addition to these compounds, studies have found that fingolimod (FTY720) is more effective against breast cancer than cisplatin. Therefore, in this study, the first examples of boron-containing derivatives of fingolimod were designed and synthesized; in addition, their structures were confirmed by spectroscopic techniques. The synthesized boron-containing drug candidates were found to significantly inhibit cell proliferation and induce apoptosis-mediated cell death in HT-29 (colorectal cells), SaOs-2 (osteosarcoma cells), and U87-MG (glioblastoma cells). Moreover, we revealed that the anticancer effects of boron-containing fingolimod compounds were found to be significantly enhanced over boron-free control groups and, strikingly, over the widely used anticancer drug 5-fluorouracil. The metabolomic analysis confirmed that administration of the boron-containing drug candidates induces significant changes in the metabolite profiles in HT-29, SaOs-2, and U87-MG cells. Altogether, our results showed that boron-containing fingolimod compounds can be further examined to reveal their potential as anticancer drug candidates.

KEYWORDS
anticancer drugs, apoptosis, boron-containing drugs, cancer, fingolimod

1 | INTRODUCTION

Boron-containing drugs exhibit advantages over conventional drugs through their mechanisms in cancer treatment. Over the past decades, researchers have developed various bioactive molecules containing boron, with a primary focus on designing protein inhibitors.[1–3] Boron, a semimetal element, possesses unique properties that make it an attractive candidate in medicinal chemistry.[4] It hybridizes sp^2 in its structure but can also hybridize sp^3 when interacting with structures, such as receptors or DNA, owing to its octet deficiency.[5] This property makes it an appealing candidate for drug development. For example, molecules containing the nonradioactive isotope ^{10}B, like boronophenylalanine, can be converted into the radioactive form ^{11}B through neutron exposure. Consequently, high energy is released, accompanied by the production of ^{4}He and ^{7}Li particles. This energy effectively destroys tumor cells and inhibits cell growth.[6]

Bortezomib (Velcade™) and ixazomib citrate (Ninlaro™) are two compounds that contain the boronic acid functional group. They

© 2023 Deutsche Pharmazeutische Gesellschaft.

were approved by the Food and Drug Administration in 2003 and 2012 for the treatment of multiple myeloma (MM). The primary inhibition mechanism for these drugs is the formation of a tetracoordinate boronate complex through coordination with the hydroxyl side chain of an active serine residue.[7]

Recent preclinical studies have revealed that fingolimod demonstrates an anticancer effect on different cancer cells due to its immunosuppressant activity. This effect has been reported in several cancer types, including leukemia, lymphoma, glioblastoma, and lung cancer.[8–11] In vitro studies of fingolimod derivatives have shown their ability to reduce the growth of tumor cells.[12]

In our previous study, we designed tetrazole-containing fingolimod-like compounds by adding tetrazole group, which is commonly used in biological studies, to the octyl group—the active site of fingolimod. Afterward, docking studies were performed using the crystal structures of hS1P1R to identify the desired derivatives that demonstrated high affinity, and these compounds were subsequently synthesized. We determined the effects of these compounds on gene expressions in SH-SY5Y, SK-N-SH, and U-118 MG cells, which yielded promising results for compounds F1-12h and F2-9.[13] In this study, we prepared boronic acid derivatives of the active substance of fingolimod and performed bioactivity studies with HT-29, SaOs-2, and U87-MG cell lines. We then used omics techniques to determine the pathways used in the mechanism of action of the compound that we believe to be the most effective (Figure 1).

2 | RESULTS AND DISCUSSION

2.1 | Chemistry

FTY720 has been studied for its anticancer effects due to its active compound fingolimod, which is an immunosuppressant. The first in vitro example of fingolimod's application was the use of boronic acid esters for cancer treatment.

Boronic acid group containing compounds, such as ixazomib or bortezomib, have been previously demonstrated to treat MM effectively.[14,15] That being the case, this study aims to synthesize tetrazole and boronic acid/ester group containing derivatives of fingolimod and test the potentials of these compounds as anticancer drug candidates on HT-29 (colorectal cells), SaOs-2 (osteosarcoma cells), and U87-MG (glioblastoma cells) cell lines.

In this study, 29 novel compounds (9 final and 20 intermediates) were synthesized, and their structures were characterized by FT-IR, ^{1}H NMR, ^{13}C APT NMR, HRMS, and X-ray diffraction spectroscopy (BF8a, Figure 2, Scheme 1).

The stereochemistry of drug-active compounds plays a significant role in docking and pharmaceutical studies. Alkylation reactions of tetrazoles produce two different regioisomers, which occur in different ratios in the reaction mixture. To determine the structure of the major product BF5 derivative compounds, BF5a was obtained through a single crystal, which was elucidated by X-ray diffraction spectroscopy.[16] The reaction of pinacol borane addition to BF5 in the presence of silver acetate was carried out in a nitrogen atmosphere using a Schlenk tube. $H_{2(g)}$ is released during this reaction, and if $H_{2(g)}$ cannot be isolated, the silver cation is reduced to silver metal, and the reaction terminates. Thus, the Schlenk tube was used to synthesize BF6.

Boronic acids (BF7) decompose through long-term interaction with air or moisture. After dissolving the BF7 series in methanol, HRMS analyses were achieved. When the HRMS spectra of compounds BF7a, BF7b, and BF7c were analyzed, all three compounds reacted with 2 mol methanol, and the molecular ion peak appeared as the sodium cation of dimethyl boronic acid ester.[17,18] Therefore, the compounds were converted to boronic acid esters with diethanolamine to stabilize.

Diethanolamine was used as the reagent in the synthesis of BF8 series compounds. After the reaction was complete, extraction (water/ethyl acetate) was performed to separate the diethanolamine from the mixture. The FT-IR spectrum of the product showed O–H stretching bands of boronic acid. As it was thought that boronic acid esters may hydrolyze in aqueous media, the BF7a compound was added to the bioactivity studies, in addition to BF8 series compounds.

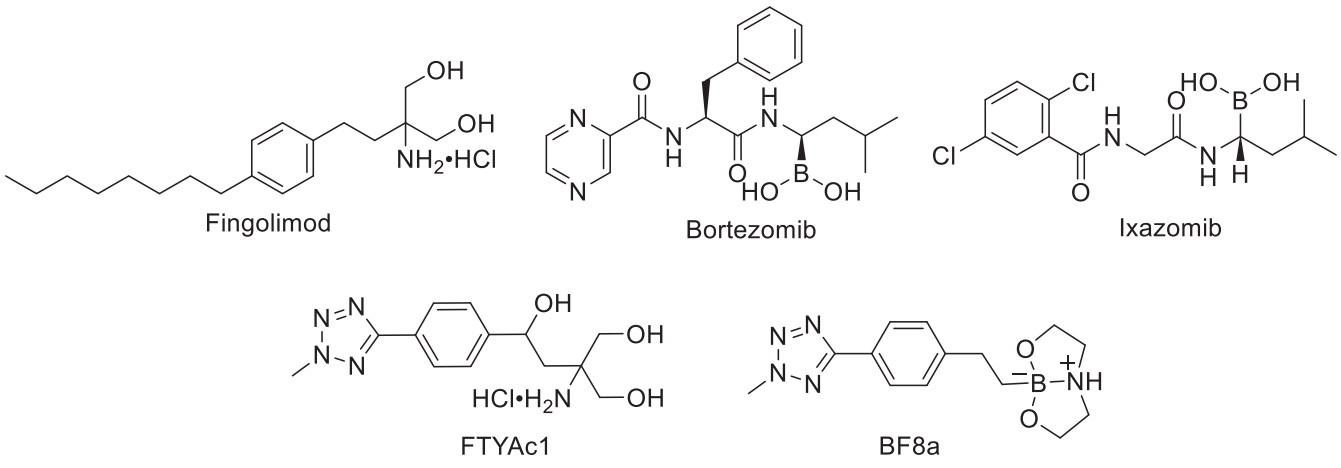


FIGURE 1 Drugs and targeted compounds in the study.

15214184, 0, Downloaded from https://onlinelibrary.wiley.com/doi/10.1002/ardp.202300382 by Gazi University, Wiley Online Library on [03/10/2023]. See the Terms and Conditions (https://onlinelibrary.wiley.com/terms-and-conditions) on Wiley Online Library for rules of use; OA articles are governed by the applicable Creative Commons License

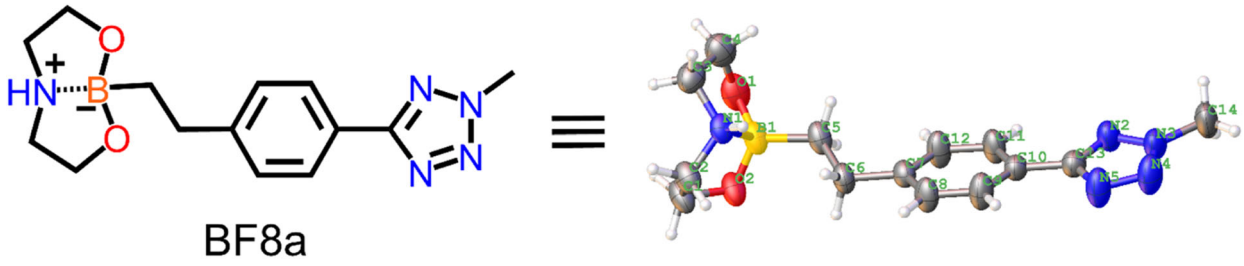
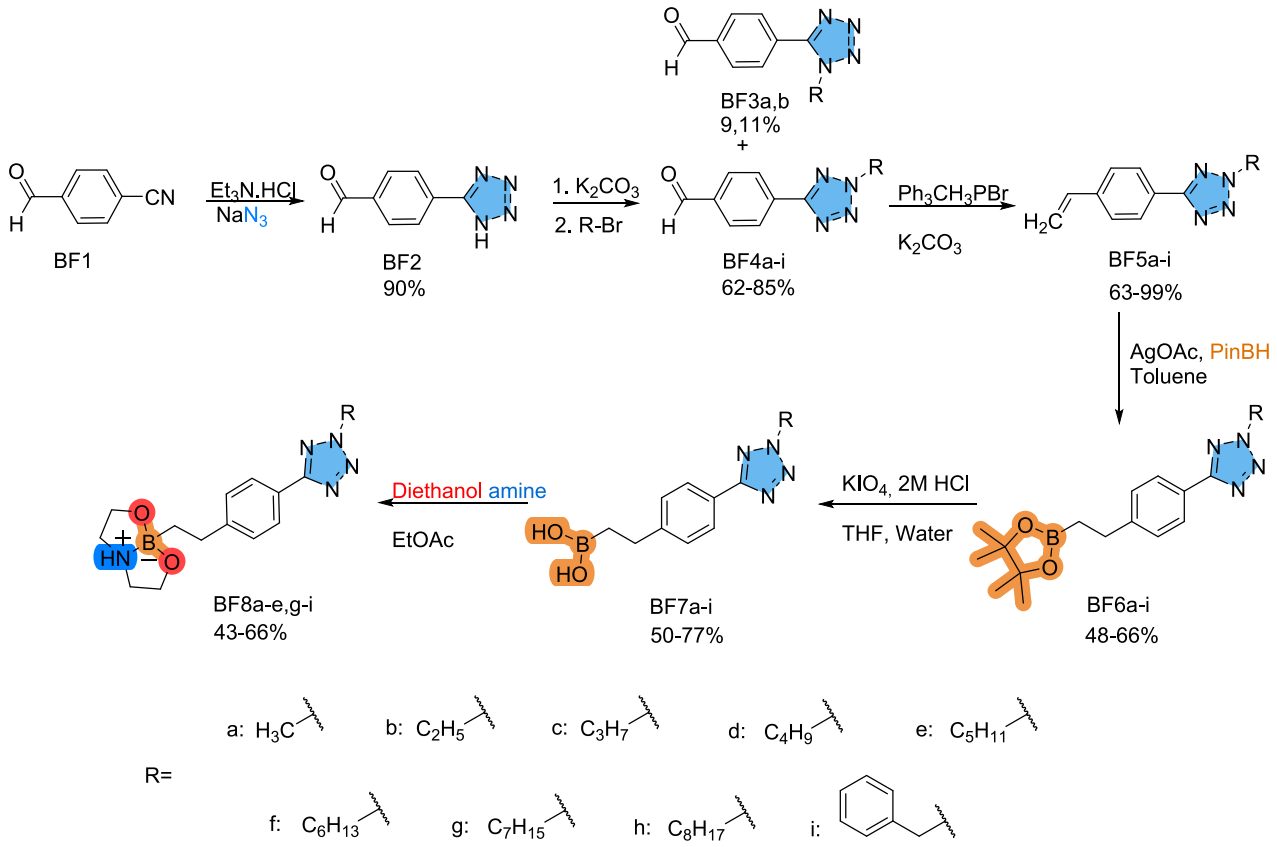


FIGURE 2 X-ray image of BF8a.



SCHEME 1 Synthetic pathways of BF series.

The structure of BF7a was clarified using X-ray diffraction spectroscopy to determine whether the boronic acid ester group of BF8 compounds has two rings or one ring. To obtain a single crystal, BF8 series compounds were crystallized using chloroform. However, despite trying different synthesis methods, such as using different solvents, stoichiometric ratios, and water adsorbers, the isolation of the BF8f compound could not be achieved (Scheme 1).

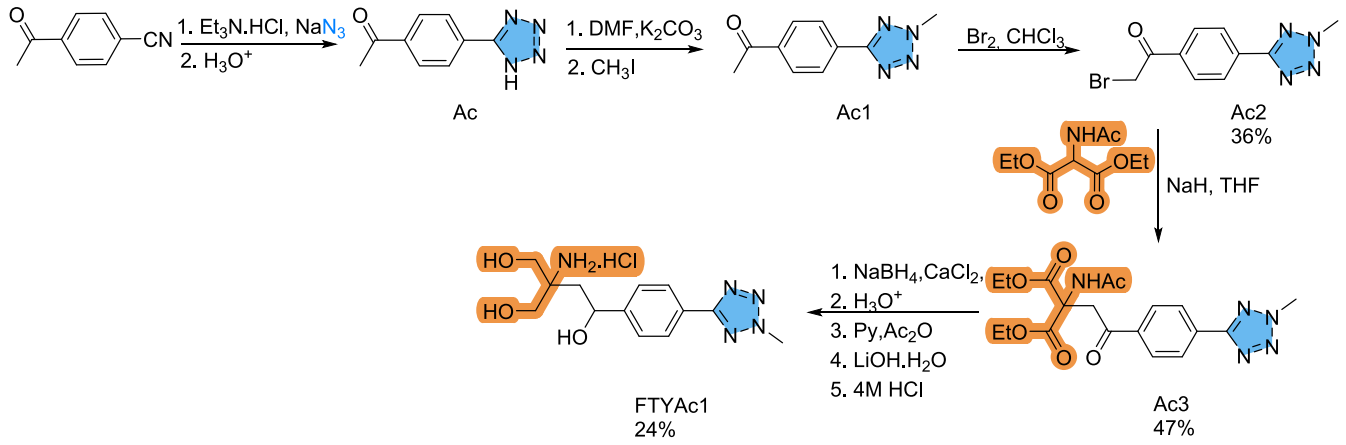
When examining the ^{13}C APT NMR spectra of all synthesized compounds containing boron atoms (BF6, BF7, and BF8 series), none of the carbons directly bonded to the boron atom were observed in the spectra. According to the literature examined, the peak of the carbons directly bonded to the boron atom is not observed in the ^{13}C APT NMR spectrum due to the quadrupole relaxation of the boron atom.[17,19]

In addition to the BF8 series compounds, a boron-free control compound (FTYAc1) was synthesized, elucidated, and used as a second control compound along with 5-fluorouracil in [2,3-bis-(2-methoxy-4-nitro-5-sulfophenyl)-2*H*-tetrazolium-5-carboxanilide] (XTT) assay studies to observe that the activity of the compounds is related to the boron atom (Scheme 2).

2.2 | Biology

To evaluate the anticancer potential of our boron-conjugated drugs on HT-29, SaOs-2, and U87-MG cells, we performed a cell proliferation test and apoptosis–necrosis test.

15214184, 0, Downloaded from https://onlinelibrary.wiley.com/doi/10.1002/ardp.202300382 by Gazi University, Wiley Online Library on [03/10/2023]. See the Terms and Conditions (https://onlinelibrary.wiley.com/terms-and-conditions) on Wiley Online Library for rules of use; OA articles are governed by the applicable Creative Commons License



SCHEME 2 Synthetic pathways of control drug (FTYAc1).

TABLE 1 The docking and XTT assay results of boron-conjugated drug-like compounds.

	HT-29 cell line (3FUG)		SaOs-2 cell line (7BMG)		U87-MG cell line (6OQI)	
	Docking score (kcal/mol)	IC_{50} (μM)	Docking score (kcal/mol)	IC_{50} (μM)	Docking score (kcal/mol)	IC_{50} (μM)
BF7a	−7.778	59.9	−5.768	37.5	−7.205	50.5
BF8a	−4.414	85.8	−4.000	28.2	−5.560	68.6
BF8b	−5.594	58.6	−3.458	49.2	−5.662	52.3
BF8c	−5.464	83.2	−3.342	55.4	−4.205	53.6
BF8d	−4.762	69.6	−4.376	59.9	−5.140	47.6
BF8e	−2.744	49.7	−3.890	56.2	−4.421	50.1
BF8g	−6.809	27.0	−4.271	45.6	−4.719	50.3
BF8h	−9.372	48.9	−4.476	45.8	−3.892	52.6
BF8i	−6.103	73.9	−3.635	52.0	−4.911	50.2
FTYac1	−5.556	>100.0	−6.011	>100.0	−7.534	>100.0
5′FU	−3.655	>100.0	−4.449	>100.0	−5.942	>100.0
2E3[a]	−14.140		-		-	
U3Z[a]	-		−11.119		-	
N14[a]	-		-		−11.982	

Abbreviation: XTT, [2,3-bis-(2-methoxy-4-nitro-5-sulfophenyl)-2*H*-tetrazolium-5-carboxanilide].

[a]Native ligand of co-crystals.

Phase-contrast microscopy results of the HT-29 cells treated with nine boron-conjugated drugs (listed in Table 1) along with negative control (drug without boron) and positive control (5-fluorouracil [5′FU]) showed that increased level (10, 20, 50, and 100 μg/mL) of boron-conjugated drugs mostly caused inhibition of the cell proliferation in HT-29 colorectal cancer cells when compared to negative control and even 5′FU for either 72 or 120-h of treatment (Supporting Information: Figures S1–S6A). XTT results supported these observations and confirmed that HT-29 cells significantly respond to the applied drug dose (Supporting Information: Figure S6B). It was easily interpreted that even with 72 h of boron-conjugated drug treatments, the cell proliferation level of HT-29 cells was decreased with increasing doses of boron-containing compounds, compared to the compound without boron and 5′FU, as shown in Figure 3a. Strikingly, 50 and 100 μg/mL of boron-conjugated drugs severely reduced the level of cell proliferation in HT-29 cells after 120 h of treatment, compared to the same doses of control and 5′FU (Figure 3a). To investigate the mechanism of the anticancer efficiency of the compounds, we then carried out an apoptosis-necrosis assay using boron-conjugated BF8a drug (20 μg/mL), which was selected considering the XTT assay. It should also be noted that BF8a has the maximum anticancer effect with 72-h of treatment period. In HT-29 cells,

15214184, 0, Downloaded from https://onlinelibrary.wiley.com/doi/10.1002/ardp.202300382 by Gazi University, Wiley Online Library on [03/10/2023]. See the Terms and Conditions (https://onlinelibrary.wiley.com/terms-and-conditions) on Wiley Online Library for rules of use; OA articles are governed by the applicable Creative Commons License

apoptosis-necrosis was visualized after 72 h of drug treatment. Cells with no drug administration were considered as a negative control, while the cells treated with 5-FU (100 µg/mL) were used as a positive control. Apoptotic cells were stained green with Apopxin Green, necrotic cells were stained red with 7-aminoactinomycin-D (7-AAD), and the cytoplasm of the living cells was stained blue with Cytocalcein Violet 450. When compared to the apoptotic (2.9%) and necrotic (2.54%) negative control group, the ratio of apoptotic (23.53%) and necrotic (15.38%) HT-29 cells was significantly increased in response to the boron-conjugated drug (Figure 3b,c).

In U87-MG cells, phase-contrast microscopy results demonstrated that increased levels (10, 20, 50, and 100 µg/mL) of boron-conjugated drugs effectively inhibited the cell proliferation in U87-MG glioblastoma cells when compared to negative control as well as positive control at both 72- and 120-h of drug treatment (Supporting Information: Figures S7–S12A). XTT results further confirmed a significant drug dose response for all drugs in U87-MG cells (Supporting Information: Figure S12B). Utilizing the heatmap (Figure 4a), it was deciphered that the cell proliferation level of glioblastoma cells was severely reduced with the increasing dose of boron-conjugated drug treatments, compared to

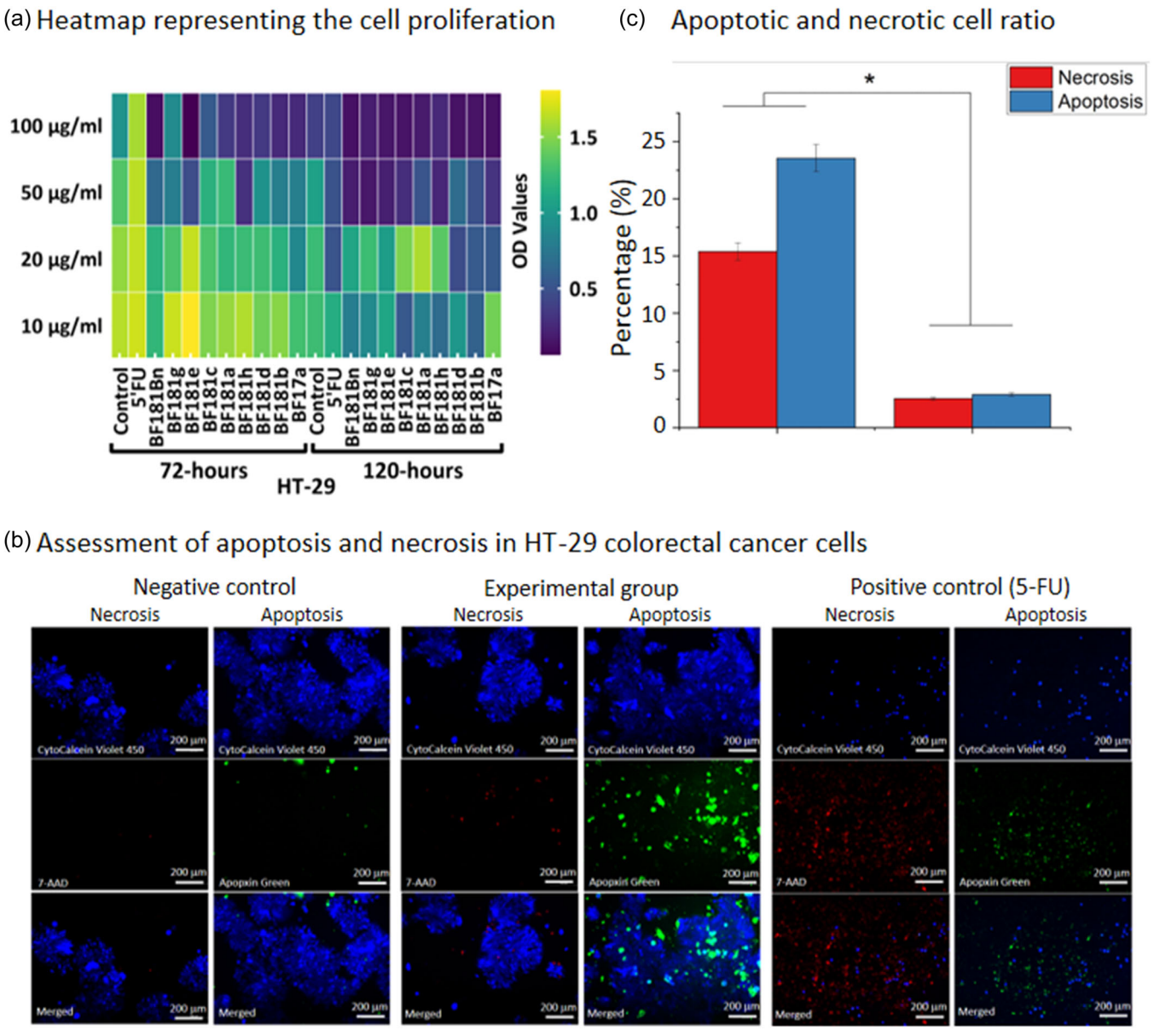
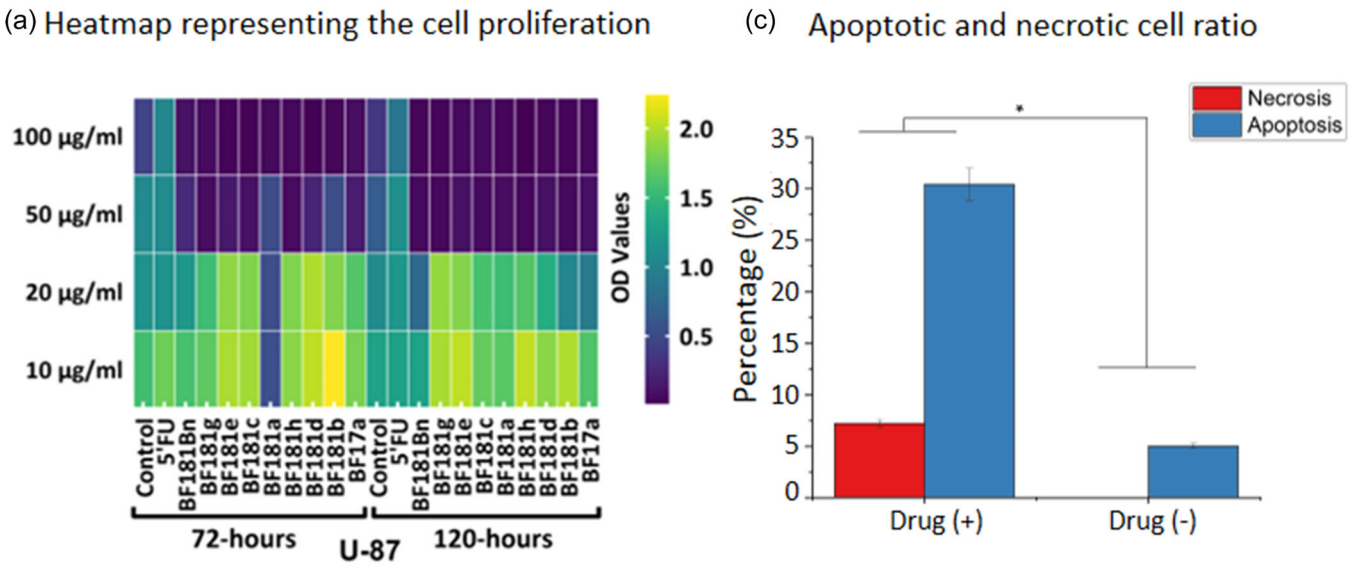


FIGURE 3 Boron-conjugated BF8a drug-mediated apoptosis in colorectal cells. (a) The heatmap summarizing the [2,3-bis-(2-methoxy-4-nitro-5-sulfophenyl)-2*H*-tetrazolium-5-carboxanilide] cell proliferation assay of HT-29 cells with different doses of the compounds compared to negative control (compound without boron) and positive control (5′FU). Student's *t* test was used to analyze comparisons between two groups as drug treatment and without drug treatment, $^{*}p < 0.05$. (b) The live cells (Blue, CytoCalcein Violet 450), apoptosis (Green, Apopxin Green), and necrosis (Red, 7-AAD) (scale bars, 200 µm). (c) The percentage of apoptosis and necrosis was determined for cells with and without drug treatment, using fluorescent microscope images (10 images were used for each group). Cells were treated with BF8a (20 µg/mL) for 72 h.

15214184, 0, Downloaded from https://onlinelibrary.wiley.com/doi/10.1002/ardp.202300382 by Gazi University, Wiley Online Library on [03/10/2023]. See the Terms and Conditions (https://onlinelibrary.wiley.com/terms-and-conditions) on Wiley Online Library for rules of use; OA articles are governed by the applicable Creative Commons License



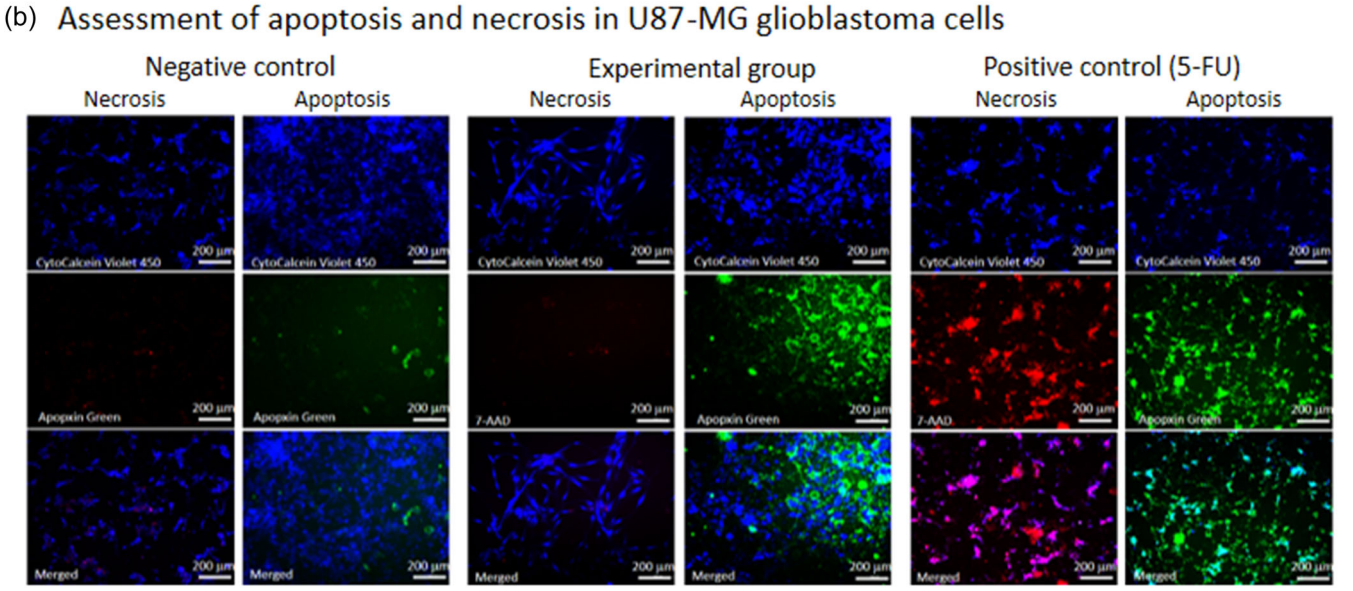


FIGURE 4 Boron-conjugated BF8a drug-mediated apoptosis in glioblastoma cells. (a) The heatmap summarizing the [2,3-bis-(2-methoxy-4-nitro-5-sulfophenyl)-2*H*-tetrazolium-5-carboxanilide] cell proliferation assay for U87-MG with different doses of the compounds compared to negative control (compound without boron) and positive control (5′FU). Student's *t* test was used to analyze comparisons between two groups as drug treatment and without drug treatment, $^*p < 0.05$. (b) The live cells (Blue, CytoCalcein Violet 450), apoptosis (Green, Apopxin Green), and necrosis (Red, 7-AAD) (scale bars, 200 µm). (c) The percentage of apoptosis and necrosis was determined for cells with and without drug treatment, using fluorescent microscope images (10 images were used for each group). Cells were treated with BF8a (20 µg/mL) for 72 h.

the negative and positive control groups after both 72- and 120-h of treatments. Similar to the results obtained with HT-29 cells, the level of necrotic cells (0%) and apoptotic control (5%) were increased in the drug-applied group, and the levels of apoptotic cells was increased to 30.43% while the level of necrotic cells slightly increased to 7.21% (Figure 4b,c).

In SaOs-2 cells, phase-contrast microscopy results displayed that increased levels (10, 20, 50, and 100 µg/mL) of boron-conjugated drugs yielded an inhibition of the cell proliferation in osteosarcoma cells (Supporting Information: Figures S13–S18A), which were confirmed quantitatively by XTT testing (Figure S18B). The obtained heatmap representing the XTT results enabled us to conclude that the cell proliferation level of SaOs-2 osteosarcoma cells was decreased even at the 72-h of boron-conjugated drug treatments, compared to the negative and positive controls (Figure 5a). Apoptotic and necrotic cells were visualized after 72 h of drug treatment. When compared to the nontreated apoptotic (2.85%) and necrotic (6.74%) group, apoptotic (17.5%) and necrotic (12.6%) SaOs-2 cells were significantly increased in response to the boron-conjugated drug (Figure 5b,c).

Altogether, our results suggest that the boron-conjugated drugs can induce a severe inhibition of cell proliferation in colorectal cells, glioblastoma cells, and osteosarcoma cells, as well as result in a cell death mediated by apoptosis pathway. We found that these

15214184, 0, Downloaded from https://onlinelibrary.wiley.com/doi/10.1002/ardp.202300382 by Gazi University, Wiley Online Library on [03/10/2023]. See the Terms and Conditions (https://onlinelibrary.wiley.com/terms-and-conditions) on Wiley Online Library for rules of use; OA articles are governed by the applicable Creative Commons License

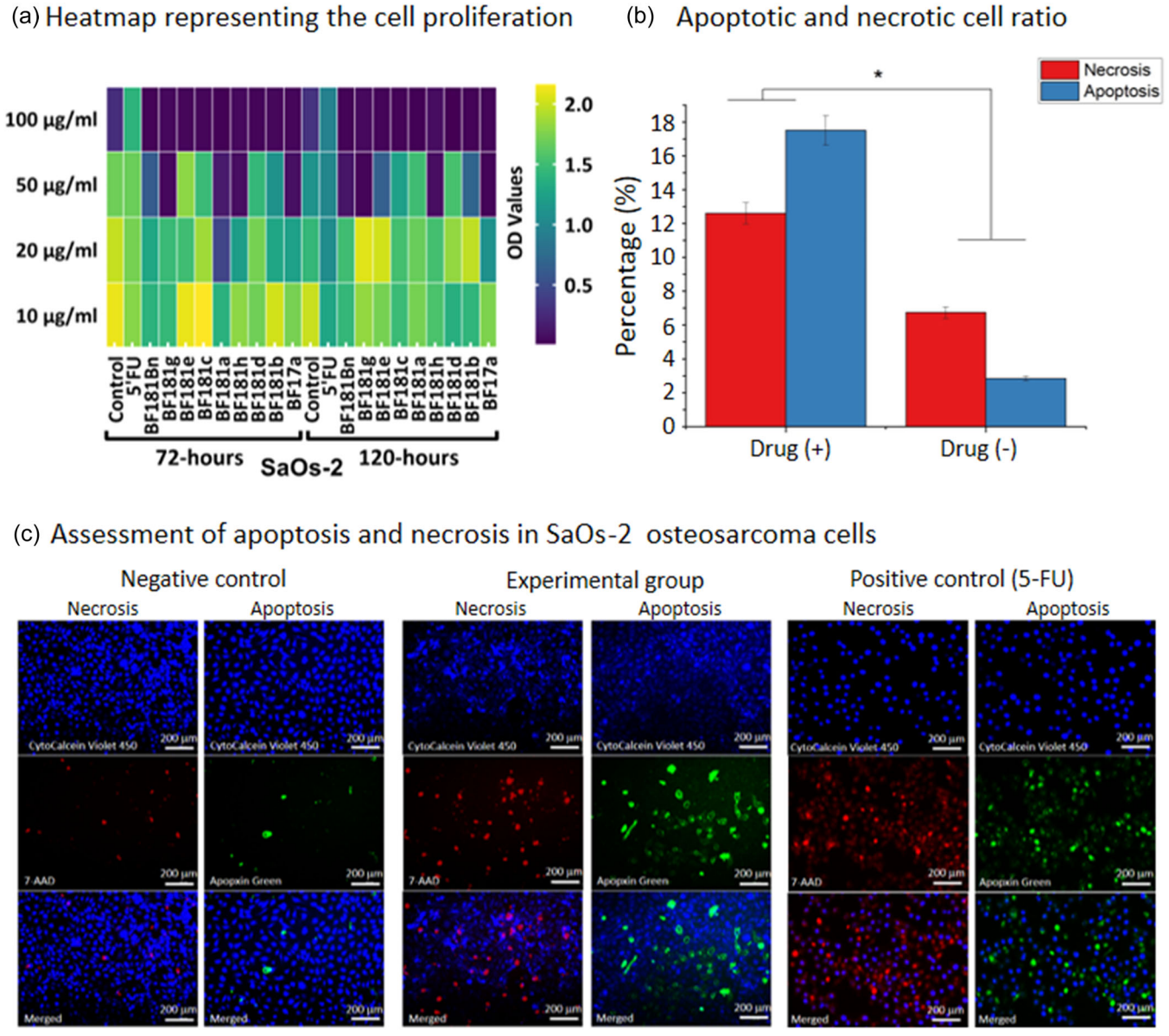


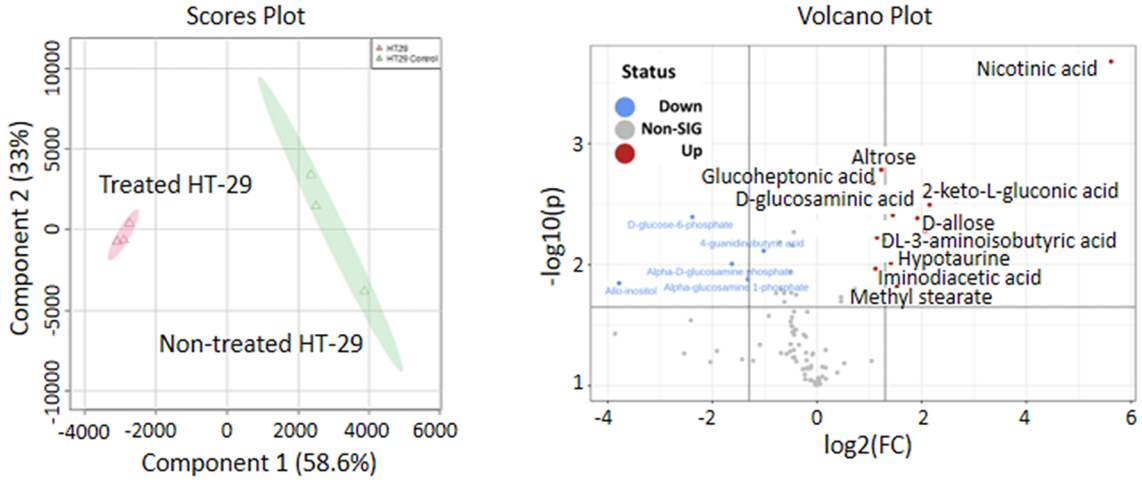
FIGURE 5 Boron-conjugated BF8a drug-mediated apoptosis in osteosarcoma cells. (a) The heatmap summarizing the [2,3-bis-(2-methoxy-4-nitro-5-sulfophenyl)-2*H*-tetrazolium-5-carboxanilide] cell proliferation assay for SaOs-2 with different doses of the compounds compared to negative control (compound without boron) and positive control (5′FU). Student's *t* test was used to analyze comparisons between two groups as drug treatment and without drug treatment, $^*p < 0.05$. (b) The live cells (Blue, CytoCalcein Violet 450), apoptosis (Green, Apopxin Green), and necrosis (Red, 7-AAD) (scale bars, 200 µm). (c) The percentage of apoptosis and necrosis was determined for cells with and without drug treatment, using fluorescent microscope images (10 images were used for each group). Cells were treated with BF8a (20 µg/mL) for 72 h.

efficiencies were significantly enhanced in BF8a when compared to the boron-free control group, and more importantly, to the commonly used anticancer drug 5′FU.

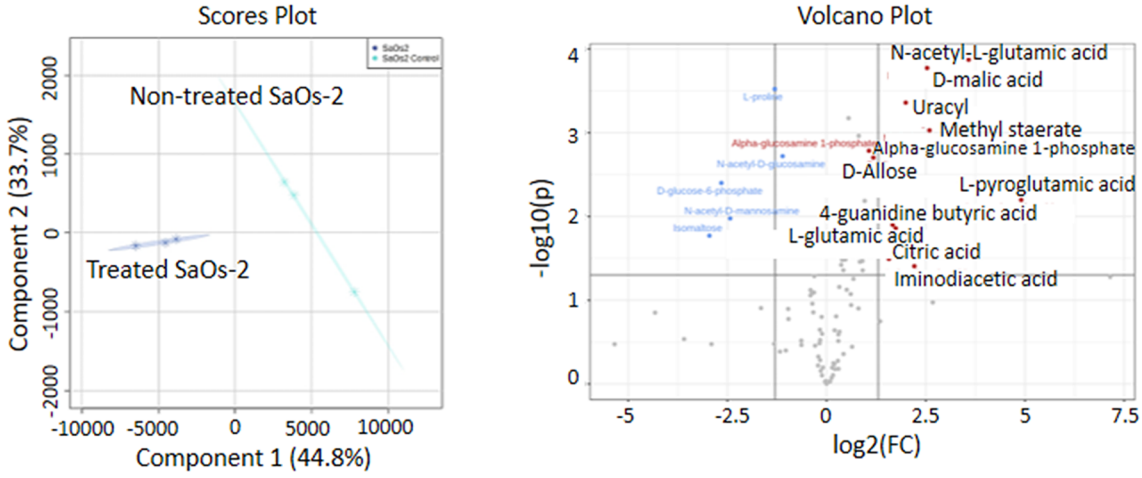
To investigate the effect of our boron-conjugated drugs on metabolic reprogramming in colorectal adenocarcinoma, glioblastoma, and osteosarcoma cells, we performed gas chromatography-mass spectrometry (GC-MS)-based metabolomics study for each cancer cell type with and without boron-conjugated BF8a drug treatment (20 µg/mL) for 72-h. The partial least squares discriminant analysis (PLS-DA) score plots showed clear discrimination between the metabolic phenotypes between control groups without treatment and cancer cells with drug treatment (Figure 6a–c). To elaborate on the differentially regulated metabolites between treated and nontreated groups, the up- and downregulated metabolites were visualized on the volcano plot of HT-29 cells (Figure 6a). We observed that energy metabolism and pentose-phosphate metabolism-related metabolites (i.e., nicotinic acid, D-allose, D-altrose, 2-keto-L-gluconic acid, citric acid, glucoheptonic acid) as well as amino acid metabolism-related metabolites (i.e., D-glucosaminic acid, DL-3-aminoisobutyric acid, hypotaurine, iminodiacetic acid) were upregulated in the BF8a-treated HT-29 cells as compared to control. In SaOs-2 cells, we revealed that protein and amino acid metabolism-related (i.e., *N*-acetyl-L-glutamic acid,

15214184, 0, Downloaded from https://onlinelibrary.wiley.com/doi/10.1002/ardp.202300382 by Gazi University, Wiley Online Library on [03/10/2023]. See the Terms and Conditions (https://onlinelibrary.wiley.com/terms-and-conditions) on Wiley Online Library for rules of use; OA articles are governed by the applicable Creative Commons License

(a) Effect of boron-conjugated drug on the metabolism of HT-29 colorectal cancer cells compared to non-treated control cells



(b) Effect of boron-conjugated drug on the metabolism of SaOs-2 osteosarcoma cells compared to non-treated control cells



(c) Effect of boron-conjugated drug on the metabolism of U87-MG glioblastoma cells compared to non-treated control cells

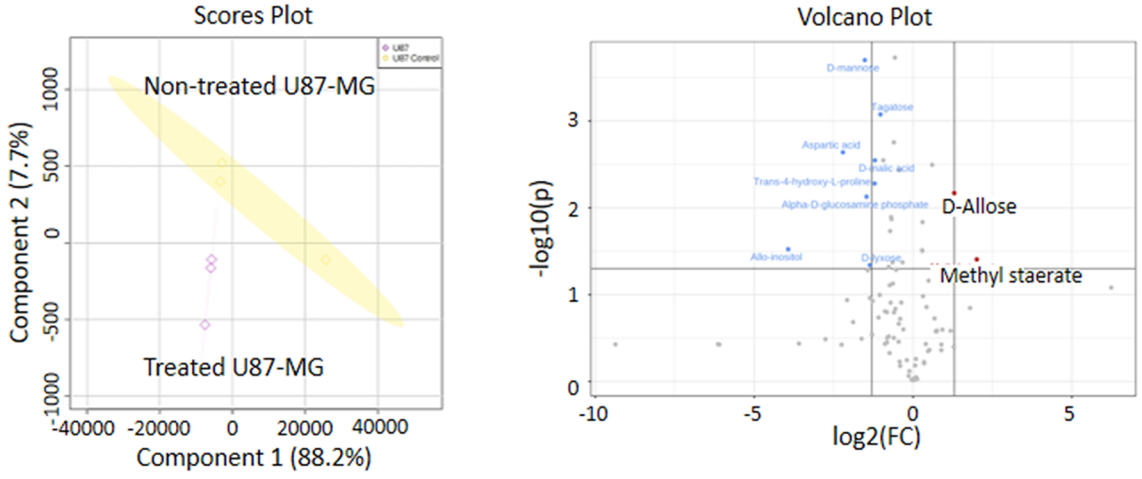


FIGURE 6 (See caption on next page).

15214184, 0, Downloaded from https://onlinelibrary.wiley.com/doi/10.1002/ardp.202300382 by Gazi University, Wiley Online Library on [03/10/2023]. See the Terms and Conditions (https://onlinelibrary.wiley.com/terms-and-conditions) on Wiley Online Library for rules of use; OA articles are governed by the applicable Creative Commons License

alpha-ketoglutaric acid, alpha-glucosamine-1-phosphate, L-pyroglutamic acid, alpha-D-glucosamine phosphate, 4-guadinobutyric acid, iminodiacetic acid, L-glutamic acid) metabolites were significantly upregulated when compared to the control (Figure 6b). Finally, upregulation of glucose metabolism and fatty acid metabolism-related metabolites were pointed out in U87-MG cells compared to the control group (Figure 6c). Our metabolomics data confirmed that boron-conjugated drug treatment brings about alterations in the metabolism of HT-29 colorectal cancer cells, SaOs-2 osteosarcoma cells, and U87-MG glioblastoma cells.

A distinct pattern of altered metabolites across whole groups was presented with a heatmap with hierarchical cluster analysis (Figure 7a). The pathway impact analysis of drug-treated HT-29 cells indicated that glycolysis/gluconeogenesis, citrate cycle, alanine, aspartate and glutamate metabolism, arginine proline metabolism, and taurine hypotaurine metabolism were reprogrammed after boron-conjugated drug treatment (Figure 7b). The pathway impact analysis of drug-treated SaOs-2 cells showed that alanine, aspartate, and glutamate metabolism, arginine biosynthesis, D-glutamine, and D-glutamate metabolism, and phenylalanine, tyrosine and tryptophan biosynthesis were reprogrammed after the treatment of boron-conjugated drug (Figure 7c). The pathway impact analysis of drug-treated U87-MG cells demonstrated that phenylalanine, tyrosine, and tryptophan biosynthesis as well as aminoacyl-tRNA biosynthesis were reprogrammed after boron-conjugated drug treatment (Figure 7d).

It can be concluded that the metabolic reprogramming of arginine biosynthesis, alanine, aspartate, and glutamate metabolism with glutamine depletion related to cellular death, and phenylalanine, tyrosine, and tryptophan biosynthesis pathway was related to increased cellular proliferation in the control cells.[20–22] After drug treatment, aminoacyl-tRNA biosynthesis can inhibit tumorigenesis by regulating apoptotic sensitivity of cancer cells[23]; citrate cycle is considered to play a crucial role in cancer metabolism as it regulates deregulated tumor suppressor expression in cancer cells,[24] and glyoxylate dicarboxylate metabolism is responsible for loss of tumor cell differentiation.[25] Glycine, serine, and threonine metabolism affect the cellular antioxidative capacity of cancer cells.[26]

2.3 | Molecular docking

This study tested the anticancer activity of a series of boronic acid/ester groups containing compounds on various cancers, that is, colon, bone, and brain cancer cell lines. Three proteins were selected for docking analysis: retinoid X receptor (colorectal cells, PDB No: 3FUG), p53-MDM2 inhibitor (osteosarcoma cells, PDB No: 7BMG), and CDK4/6 inhibitor (glioblastoma cells, PDB No: 6OQI). The docking analysis results obtained for different types of compounds are presented in Table 1.

Cell proliferation testing results depicted that BF8a was the most effective compound with an effective concentration of 20 μg/mL for all three cell lines. The interaction between BF8a and target proteins was then examined. In colorectal cells, there was a π–π stacking interaction between the PHE313 residue and the phenyl group. There was also a weak interaction between the ALA327 and ALA271 residues and the methyl hydrogens attached to the tetrazole ring. In addition, a hydrogen bond interaction was observed between the CYS432 and PHE439 residues and the boronate oxygen atom. The interaction between BF8a and target proteins (3FUG) was provided in a three-dimensional simulation in Figure 8a.

In the case of the interaction between BF8a and SaOs-2 (osteosarcoma cells), weak interactions were observed between the GLN24 residue and ethylene hydrogens in the diethanol amine group, and between residues HIE96, VAL93, and MET62 and the phenyl and methyl hydrogens attached to the tetrazole ring. These interactions between BF8a and the target protein (7BMG) are illustrated in Figure 8b.

In glioblastoma cells (U87-MG), there was a π–π stacking interaction with the PHE80 residue and the tetrazole ring. There was also a weak interaction between the ASP145 and PHE80 residues and the methyl hydrogens attached to the tetrazole ring. The simulation of the interaction between BF8a and the target protein (6OQI) is presented in Figure 8c.

3 | CONCLUSION

The synthesized boron-containing drug candidates were able to significantly inhibit cell proliferation in HT-29 (colorectal cells), SaOs-2 (osteosarcoma cells), and U87-MG (glioblastoma cells) cells and were also able to induce cell death mediated by apoptotic pathways. These effects were found to be significantly enhanced compared to the other boron-free control drug candidate group and the widely used anticancer drug 5′FU. The metabolomic analysis confirmed that the administration of boron-conjugated drug candidates caused significant changes in the metabolites of HT-29 cells, SaOs-2 cells, and U87-MG cells.

FIGURE 6 Effect of the boron-conjugated drug (BF8a) on the metabolic profiling of HT-29, SaOs-2, and U87-MG cell lines for a coculture period of 72 h. (a) Partial least squares discriminant analysis (PLS-DA) score plot that represents metabolomics discrimination between HT-29 colorectal cancer cells treated with boron-conjugated drug (BF8a) compared to nontreated control, and up- and downregulated metabolites of HT-29 colorectal cancer cells treated with boron-conjugated drug (BF8a) compared to control showed with volcano plots. (b) PLS-DA score plot that represents metabolomics discrimination between SaOs-2 osteosarcoma cells treated with boron-conjugated drug (BF8a) compared to nontreated control, and up- and downregulated metabolites of SaOs-2 osteosarcoma cells treated with boron-conjugated drug (BF8a) compared to control showed with volcano plots. (c) PLS-DA score plot that represents metabolomics discrimination between U87-MG glioblastoma cells treated with boron-conjugated drug (BF8a) compared to nontreated control, and up- and downregulated metabolites of U87-MG glioblastoma cells treated with boron-conjugated drug (BF8a) compared to control shown with volcano plots. $n = 3$ and p significance determined by Student's t test.

15214184, 0, Downloaded from https://onlinelibrary.wiley.com/doi/10.1002/ardp.202300382 by Gazi University, Wiley Online Library on [03/10/2023]. See the Terms and Conditions (https://onlinelibrary.wiley.com/terms-and-conditions) on Wiley Online Library for rules of use; OA articles are governed by the applicable Creative Commons License

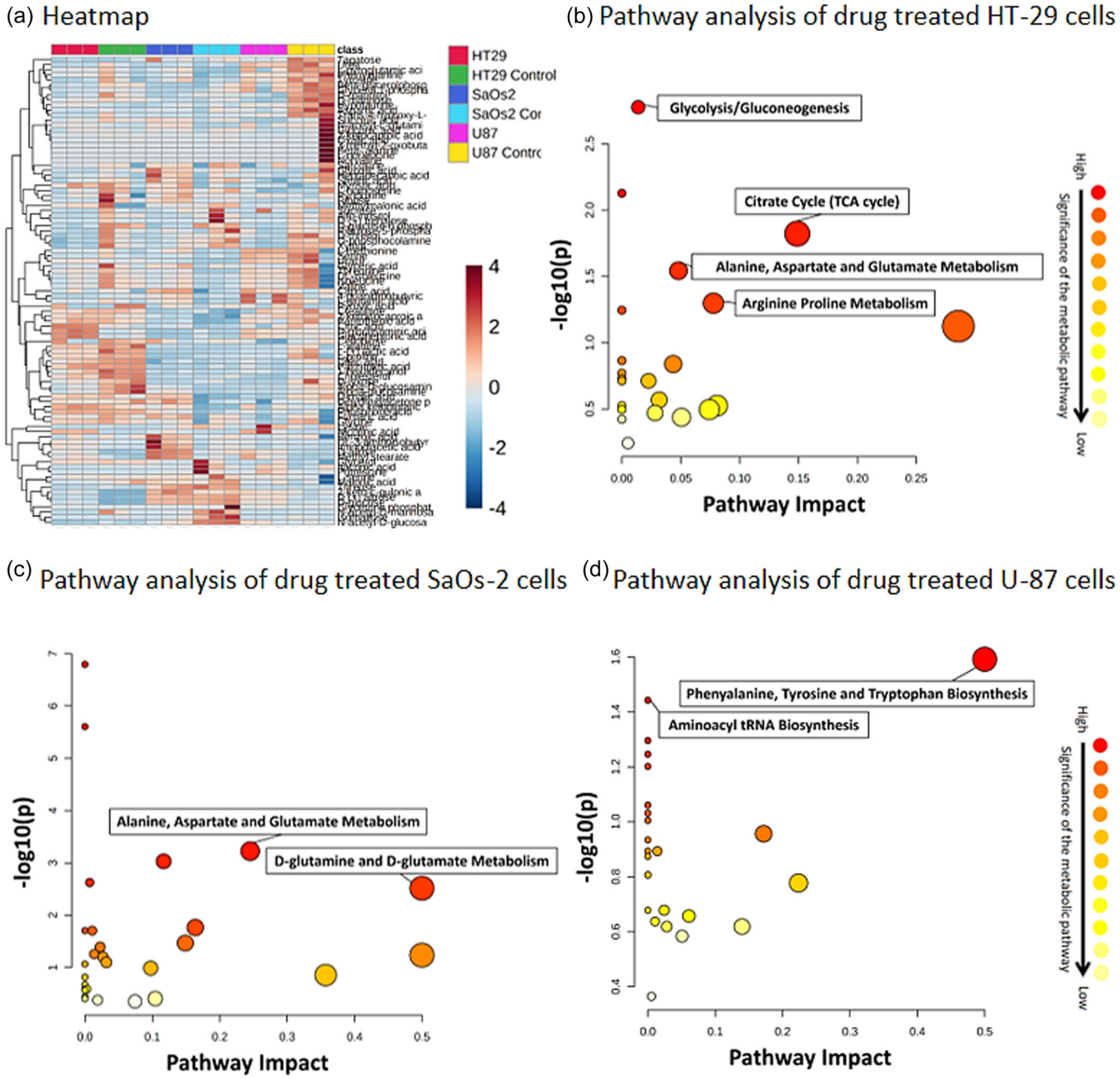


FIGURE 7 Metabolomic reprogramming and the affected pathways in cancer cells in response to the boron-conjugated drug (BF8a). (a) Heatmap with hierarchical clustering analysis obtained by most altered metabolites in the treated and nontreated HT-29, SaOs-2, and U87-MG cells. Statistical significance was determined by one-way analysis of variance. Pathway impact analysis shows the altered metabolic pathways of (b) HT-29 cells, (c) SaOs-2 cells, and (d) U87-MG cells in response to BF8a. $n = 3$, p significance was determined by Student's t test.

Furthermore, metabolomic profiling showed that the synthesized boron-containing drug candidates reprogrammed the metabolome toward an antitumourigenic and apoptotic profile in colorectal cells, osteosarcoma, and glioblastoma cells compared to the untreated group.

Several anticancer drugs have been produced to modulate programmed cell death and this offers an effective approach to treat many cancers. Therefore, drugs targeting apoptosis are seen as a promising strategy in anticancer drug discovery. Necrotic cell death is the type of death favored by cells when a cell cannot die through apoptosis at low energy levels and under high-stress conditions. Swelling of cells, rupture of the cell membrane, and expulsion of cell contents are the consequences of necrotic cell death. These conditions can be harmful to other cells in their environment. For this reason, apoptosis is considered to be a more favored approach than necrosis in cancer treatment and anticancer drug discovery research. The synthesized compounds were found to induce cellular death primarily through apoptosis. As a result, it is thought that these synthesized boron-containing compounds can be used as anticancer drugs.

It is known that widely used drugs, such as 5′FU, bind to nucleic acids, affect cell cycle phases, and consequently halt the proliferation of

15214184, 0, Downloaded from https://onlinelibrary.wiley.com/doi/10.1002/ardp.202300382 by Gazi University, Wiley Online Library on [03/10/2023]. See the Terms and Conditions (https://onlinelibrary.wiley.com/terms-and-conditions) on Wiley Online Library for rules of use; OA articles are governed by the applicable Creative Commons License

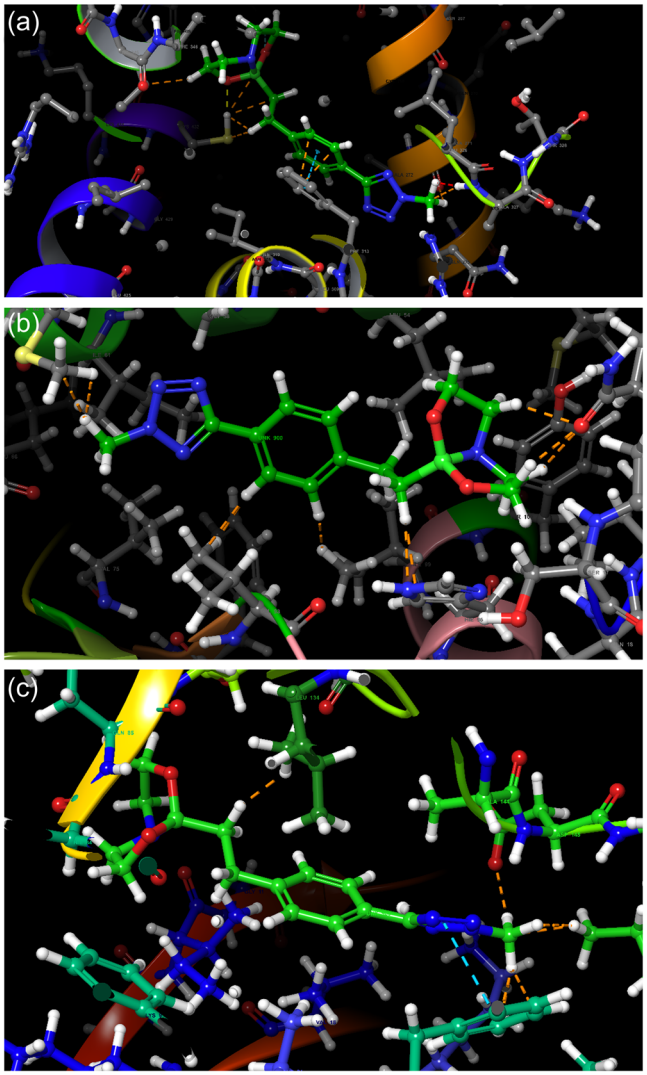


FIGURE 8 Three-dimensional interaction of compounds with BF8a with target proteins (a) 3FUG, (b) 7BMG, and (c) 6OQI.

cancer cells. On the other hand, the presented boron-containing fingolimod derivatives in this study act as inhibitors for both S1P receptors and protein kinase C, thereby halting cancer cell proliferation in this way. By inhibiting these pathways, they induce cancer cell apoptosis, as demonstrated in this study. In conclusion, fingolimod derivatives induce cancer apoptosis through a different mechanism than 5-FU; the potential adverse effects of these mechanisms should be thoroughly investigated in future studies.

4 | EXPERIMENTAL

4.1 | Chemistry

4.1.1 | General

All chemicals, glass equipment, solvents, and reagents used in the syntheses were purchased from commercially available sources. Since the chemicals used were of sufficient purity, no further purification was performed. The toluene used in the BF6 step was kept for a day after adding dry sodium sulfate. The structures of the BF3/BF4/BF5 series and Ac1 were elucidated in our previous study (Scheme 2).[16] The reactions were monitored using silica-gel-coated ($60F_{254}$) thin-layer chromatography (TLC) aluminum plates, and the spots were observed using a UV lamp. Purification of the compounds was carried out by flash chromatography on a Buechi C-601 column with ISOLAB silica gel (230–400 Mesh). FT-IR spectra were taken using a Thermo Nicolet ID5 ATR at the Gazi University Chemistry Department. ^{1}H and ^{13}C NMR spectra were acquired using a 300 MHz Bruker Avance Ultrashield NMR system, and the chemical shifts were reported relative to the solvent peak. HRMS analyses were performed using Agilent LC/MS-High Resolution Quadrupole Mass Time-of-Flight (Q-TOF) with electrospray ionization at Bilkent University National Nanotechnology Research Center.

The InChI codes of the investigated compounds, together with some biological activity data, are provided as Supporting Information.

4.1.2 | General procedure for the synthesis of 2-alkyl-5-{4-[2-(4,4,5,5-tetramethyl-1,3,2-dioxaborolan-2-yl)ethyl]phenyl}-2*H*-tetrazole (**BF6a–i**)

The synthesis procedure of Wang et al. was performed with some modifications. The appropriate vinyl tetrazole derivative (1 equiv), AgOAc (0.1 equiv), PinBH (1.5 equiv), and 1 mL of toluene dried with sodium sulfate was quickly added into a flame-dried Schlenk tube in an N_2 atmosphere and sealed. The mixture was heated for 24 h at 110°C (the temperature of the oil bath). The reaction mixture was diluted with DCM (5 mL) and filtered, and the solvents were removed using a rotary evaporator under reduced pressure. The product was purified by flash chromatography using hexane/ethyl acetate in the appropriate ratio.[27]

*2-Methyl-5-{4-[2-(4,4,5,5-tetramethyl-1,3,2-dioxaborolan-2-yl) ethyl]phenyl}-2H-tetrazole (**BF6a**)*

120.3 mg (66%) of white powder; m.p. 62–65°C. ^{1}H NMR ($CDCl_3$): $\delta = 8.02$ (d, 2H, $J = 8.1$ Hz) –CH, 7.34 (d, 2H, $J = 8.0$ Hz) –CH, 4.37 (b, 3H) $-CH_3$, 2.81 (t, 2H, $J = 8.1$ Hz) $-CH_2$, 1.50–1.00 (14H) $-CH_3$, $-CH_2$; ^{13}C NMR ($CDCl_3$): δ = 165.4, 146.9, 128.5, 126.6, 124.6, 83.1, 39.9, 29.9, 24.8. HRMS(ESI): $[M+H]^+$ calculated for $C_{16}H_{24}BN_4O_2$ 315.1987, found: 315.1376. IR: υ 3024 and 2979 cm^{-1}.

*2-Ethyl-5-{4-[2-(4,4,5,5-tetramethyl-1,3,2-dioxaborolan-2-yl)ethyl] phenyl}-2H-tetrazole (**BF6b**)*

157.5 mg (48%) of colorless liquid; ^{1}H NMR ($CDCl_3$): $\delta = 8.04$ (d, 2H, $J = 8.0$ Hz) –CH, 7.34 (d, 2H, $J = 8.0$ Hz) –CH, 4.69 (q, 2H, $J = 7.3$ Hz) $-CH_2$, 2.81 (t, 2H, $J = 8.0$ Hz) $-CH_2$, 1.68 (t, 3H) $-CH_3$, 1.25–1.20 (m, 14H) $-CH_3$, $-CH_2$; ^{13}C NMR ($CDCl_3$): $\delta = 165.2$, 146.8, 128.5, 126.6, 124.8, 83.1, 48.2, 29.8, 24.7, 14.5. HRMS (ESI): $[M+H]^+$ calculated for $C_{17}H_{26}BN_4O_2$ 329.2149, found: 329,2146. IR: υ 3035 and 2976 cm^{-1}.

15214184, 0, Downloaded from https://onlinelibrary.wiley.com/doi/10.1002/ardp.202300382 by Gazi University, Wiley Online Library on [03/10/2023]. See the Terms and Conditions (https://onlinelibrary.wiley.com/terms-and-conditions) on Wiley Online Library for rules of use; OA articles are governed by the applicable Creative Commons License

*2-Propyl-5-{4-[2-(4,4,5,5-tetramethyl-1,3,2-dioxaborolan-2-yl) ethyl]phenyl}-2H-tetrazole (**BF6c**)*

210.0 mg (66%) of colorless liquid; ^{1}H NMR ($CDCl_3$) δ = 8.03 (d, 2H, J = 8.1 Hz) –CH, 7.33 (d, 2H, J = 8.1 Hz) –CH, 4.59 (t, 2H, J = 7.1 Hz) $-CH_2$, 2.80 (t, 2H, J = 8.0 Hz) $-CH_2$, 2.15–2.00 (m, 2H) $-CH_2$, 1.50–1.00 (m, 14H) $-CH_3$, $-CH_2$, 0.99 (t, 3H, J = 7.4 Hz) $-CH_3$; ^{13}C NMR ($CDCl_3$): δ = 165.1, 146.8, 128.5, 126.6, 124.8, 83.1, 54.6, 29.8, 24.7, 22.8, 10.9. HRMS (ESI): $[M+Na]^+$ calculated for $C_{18}H_{27}BN_4NaO_2$ 365.2125, found: 365.2117. IR: υ 3026 and 2974 cm^{-1}.

*2-Butyl-5-{4-[2-(4,4,5,5-tetramethyl-1,3,2-dioxaborolan-2-yl)ethyl] phenyl}-2H-tetrazole (**BF6d**)*

105.4 mg (51%) of colorless liquid; ^{1}H NMR ($CDCl_3$): δ = 8.04 (d, 2H, J = 8.2 Hz) –CH, 7.34 (d, 2H, J = 8.2 Hz) –CH, 4.64 (t, 2H, J = 7.1 Hz) $-CH_2$, 2.81 (t, 2H, J = 8.0 Hz) $-CH_2$, 2.10–1.95 (m, 2H) $-CH_2$, 1.40–1.10 (m, 14H) $-CH_3$, $-CH_2$, 0.98 (t, 2H, J = 7.3 Hz) $-CH_2$, 0.95–0.85 (t, 3H) $-CH_3$; ^{13}C NMR ($CDCl_3$): δ = 165.1, 146.8, 128.5, 126.6, 124.9, 83.1, 52.7, 31.0, 29.9, 24.7, 19.6, 13.3. HRMS (ESI): $[M+Na]^+$ calculated for $C_{19}H_{29}BN_4NaO_2$ 379.2276, found: 379.2285. IR: υ 3075 and 2924 cm^{-1}.

*2-Pentyl-5-{4-[2-(4,4,5,5-tetramethyl-1,3,2-dioxaborolan-2-yl) ethyl]phenyl}-2H-tetrazole (**BF6e**)*

190.0 mg (54%) of colorless liquid; ^{1}H NMR ($CDCl_3$): δ = 8.03 (d, 2H, J = 8.1 Hz) –CH, 7.33 (d, 2H, J = 8.0 Hz) –CH, 4.62 (t, 2H, J = 7.1 Hz) $-CH_2$, 2.80 (t, 2H, J = 8.0 Hz) $-CH_2$, 2.1–2.00 (m, 2H) -CH_2, 1.50–1.00 (m, 18H) $-CH_3$, $-CH_2$, 0.89 (t, 3H, J = 7.0 Hz) $-CH_3$; ^{13}C NMR ($CDCl_3$): δ = 165.1, 146.8, 128.5, 126.6, 124.7, 83.2, 53.1, 29.9, 29.0, 28.4, 21.9, 24.7, 13.8. HRMS (ESI): $[M+H]^+$ calculated for $C_{20}H_{32}BN_4O_2$ 371.2613, found: 371.2640. IR: υ 3028 and 2955 cm^{-1}.

*2-Hexyl-5-{4-[2-(4,4,5,5-tetramethyl-1,3,2-dioxaborolan-2-yl)ethyl] phenyl}-2H-tetrazole (**BF6f**)*

229.7 mg (49%) of colorless liquid; ^{1}H NMR ($CDCl_3$): δ = 8.04 (d, 2H, J = 8.1 Hz) –CH, 7.34 (d, 2H, J = 8.0 Hz) –CH, 4.63 (t, 2H, J = 7.1 Hz) $-CH_2$, 2.81 (t, 2H, J = 8.0 Hz) $-CH_2$, 2.15–2.00 (m, 2H) $-CH_2$, 1.50–1.00 (m, 20H) $-CH_3$, $-CH_2$, 1.00–0.85 (t, 3H) $-CH_3$; ^{13}C NMR ($CDCl_3$): δ = 165.1, 146.8, 128.5, 126.6, 124.8, 83.1, 53.1, 31.0, 29.9, 29.7, 26.0, 24.8, 22.3, 13.9. HRMS (ESI): $[M+H]^+$ calculated for $C_{21}H_{34}BN_4O_2$ 385.2769, found: 385.2774. IR: υ 3032 and 2953 cm^{-1}.

*2-Heptyl-5-{4-[2-(4,4,5,5-tetramethyl-1,3,2-dioxaborolan-2-yl) ethyl]phenyl}-2H-tetrazole (**BF6g**)*

247.6 mg (56%) of colorless liquid; ^{1}H NMR ($CDCl_3$): δ = 8,04 (d, 2H, J = 8.2 Hz) –CH, 7.34 (d, 2H, J = 8.1 Hz) –CH, 4.63 (t, 2H, J = 7.1 Hz) $-CH_2$, 2.81 (t, 2H, J = 8.1 Hz) $-CH_2$, 2.15–2.00 (m, 2H) $-CH_2$, 1.50–1.10 (m, 22H) $-CH_3$, $-CH_2$, 0.90–0.80 (t, 3H) $-CH_3$; ^{13}C NMR ($CDCl_3$): δ = 165.1, 146.8, 128.5, 126.6, 124.8, 83.1, 53.1, 31.5, 29.8, 29.3, 28.5, 26.2, 24.7, 22.4, 13.9. HRMS (ESI): $[M+H]^+$ calculated for $C_{22}H_{36}BN_4O_2$ 399.2926, found: 399.2922. IR: υ 3069 and 2922 cm^{-1}.

*2-Octyl-5-{4-[2-(4,4,5,5-tetramethyl-1,3,2-dioxaborolan-2-yl)ethyl] phenyl}-2H-tetrazole (**BF6h**)*

181.8 mg (63%) of colorless liquid; ^{1}H NMR ($CDCl_3$): δ = 8.04 (d, 2H, J = 8.1 Hz) –CH, 7.34 (d, 2H, J = 8.1 Hz) –CH, 4.63 (t, 2H, J = 7.2 Hz) $-CH_2$, 2.81 (t, 2H, J = 8.1 Hz) $-CH_2$, 2.15–2.00 (m, 2H) $-CH_2$, 1.30–1.15 (m, 24H) $-CH_3$, $-CH_2$, 0.87 (t, 3H, J = 6.3 Hz) $-CH_3$; ^{13}C NMR ($CDCl_3$): δ = 165.1, 146.8, 128.5, 126.6, 124.8, 83.1, 53.1, 31.6, 29.9, 29.3, 28.9, 28.8, 26.3, 24.8, 22.5, 14.0. HRMS (ESI): $[M+H]^+$ calculated for $C_{23}H_{38}BN_4O_2$ 413.3088, found: 413.3116. IR: υ 3026 and 2956 cm^{-1}.

*2-Benzyl-5-{4-[2-(4,4,5,5-tetramethyl-1,3,2-dioxaborolan-2-yl) ethyl]phenyl}-2H-tetrazole (**BF6i**)*

186.8 mg (63%) of white solid; m.p. 122–125°C. ^{1}H NMR ($CDCl_3$): δ = 8.03 (d, 2H, J = 8.1 Hz) –CH, 7.45–7.25 (m, 7H) –CH, 5.87 (s, 2H) $-CH_2$, 2.80 (t, 2H, J = 8.0 Hz) $-CH_2$, 1.50–1.00 (m, 14H) $-CH_3$, $-CH_2$; ^{13}C NMR ($CDCl_3$): δ = 163.0, 144.4, 130.9, 126.4, 126.3, 126.0, 125.7, 124.2, 80.6, 54.1, 27.3, 22.2. HRMS (ESI): $[M+H]^+$ calculated for $C_{22}H_{28}BN_4O_2$ 391.2305, found: 391.1042. IR: υ 3030 and 2976 cm^{-1}.

4.1.3 | General procedure for the synthesis of [4-(2-alkyl-2*H*-tetrazol-5-yl)phenethyl]boronic acid (**BF7a–i**)

The synthesis procedure of Ma et al. was used with slight modifications. The appropriate pinacol borane derivative compound (1 equiv) and KIO_4 (4.5 equiv) were added to a mixture of THF/water (10.0:2.4 mL) and stirred for 5 min at room temperature, after which 2 M HCl (2 mL) was added. The mixture was monitored using hexane/ethyl acetate (1:1) on a TLC plate. Water (10 mL) was added to the reaction mixture, and extraction was carried out with ethyl acetate (3 × 15 mL). The solvent was washed with distilled water and saturated NaCl solution. The organic phase was dried with $MgSO_4$, and the solvent was removed using a rotary evaporator under reduced pressure. The remaining viscous liquid was crystallized with petroleum ether-ethyl acetate.[28]

*[4-(2-Methyl-2H-tetrazole-5-yl)phenethyl]boronic acid (**BF7a**)*

64.4 mg (77%) of white solid; m.p. 120–122°C. ^{1}H NMR ($CDCl_3$): δ = 8.06 (d, 2H, J = 8.0 Hz) –CH, 7.35 (d, 2H, J = 7.7 Hz) –CH, 4.39 (s, 3H) $-CH_3$, 4.22 (s, 1H) –OH, 2.83 (t, 2H, J = 7.9 Hz) $-CH_2$, 1.23 (t, 2H, J = 7.9 Hz) $-CH_2$; ^{13}C NMR (MeOH-d_4): δ = 166.2, 149.2, 129.6, 127.6, 125.5, 39.9, 31.2. HRMS (ESI): $[M+CH_3OH+Na-H_2O]^+$ calculated for $C_{11}H_{15}BN_4NaO_2$ 269.1186, found: 269.1210 [M+37]; $[M+2CH_3OH+Na-2H_2O]^+$ calculated for $C_{12}H_{17}BN_4NaO_2$ 283.1342, found: 283.1345 [M+51]. IR: υ 3346, 3035, and 2926 cm^{-1}.

*[4-(2-Ethyl-2H-tetrazole-5-yl)phenethyl]boronic acid (**BF7b**)*

161.2 mg (72%) of white solid; m.p. 117–121°C. ^{1}H NMR (DMSO-d_6): δ = 7.95 (d, 2H, J = 8.2 Hz) –CH, 7.58 (s, 1H) –OH, 7.36 (d, 2H, J = 8.2 Hz) –CH, 4.73 (q, 2H, J = 7.2 Hz) $-CH_2$, 2.71 (t, 2H, J = 7.9 Hz) $-CH_2$,

15214184, 0, Downloaded from https://onlinelibrary.wiley.com/doi/10.1002/ardp.202300382 by Gazi University, Wiley Online Library on [03/10/2023]. See the Terms and Conditions (https://onlinelibrary.wiley.com/terms-and-conditions) on Wiley Online Library for rules of use; OA articles are governed by the applicable Creative Commons License

1.56 (t, 3H, J = 7.3 Hz) $-CH_3$, 0.96 (t, 2H, J = 8.1 Hz) $-CH_2$; ^{13}C NMR (DMSO-d_6): δ = 164.6, 148.2, 129.0, 126.7, 124.6, 48.5, 30.5, 14.7. HRMS (ESI): $[M+CH_3OH+Na-H_2O]^+$ calculated for $C_{12}H_{17}BN_4NaO_2$ 283.1342, found: 283.1380 [M+37]; $[M+2CH_3OH+Na-2H_2O]^+$ calculated for $C_{13}H_{19}BN_4NaO_2$ 297.1499, found: 297.1539 [M+51]. IR: υ 3351, 3042, and 2924 cm^{-1}.

*[4-(2-Propyl-2H-tetrazole-5-yl)phenethyl]boronic acid (**BF7c**)*

168.1 mg (71%) of white solid; m.p. 106–110°C. ^{1}H NMR ($CDCl_3$): δ = 8.07 (d, 2H, J = 8.0 Hz) –CH, 7.35 (d, 2H, J = 7.9 Hz) –CH, 4.62 (t, 2H, J = 7.0 Hz) $-CH_2$, 2.83 (t, 2H, J = 7.8 Hz) $-CH_2$, 2.20–2.00 (m, 2H) $-CH_2$, 1.24 (t, 2H, J = 8.1 Hz) $-CH_2$, 1.01 (t, 3H, J = 7.3 Hz) $-CH_3$; ^{13}C NMR ($CDCl_3$): δ = 165.0, 146.6, 128.4, 126.9, 124.9, 54.7, 30.1, 22.8, 10.1. HRMS (ESI): $[M+H]^+$ calculated for $C_{13}H_{19}BN_4NaO_2$ 297.1499, found: 297.1507 [M+37]; $[M+2CH_3OH+Na-2H_2O]^+$ calculated for $C_{14}H_{21}BN_4NaO_2$ 311.1655, found: 311.1664 [M+51]. IR: υ 3366 and 2925 cm^{-1}.

*[4-(2-Butyl-2H-tetrazole-5-yl)phenethyl]boronic acid (**BF7d**)*

66.7 mg (64%) of white solid; m.p. 91–95°C. ^{1}H NMR ($CDCl_3$): δ = 8.07 (d, 2H, J = 8.0 Hz) –CH, 7.34 (d, 2H, J = 8.0 Hz) –CH, 4.64 (t, 2H, J = 7.1 Hz) $-CH_2$, 4.35–4.25 (brd s, 1H) –OH, 2.82 (t, 2H, J = 7.9 Hz) $-CH_2$, 2.10–2.00 (m, 2H) $-CH_2$, 1.45–1.30 (m, 2H) $-CH_2$, 1.23 (t, 2H, J = 8.0 Hz) $-CH_2$, 0.98 (t, 3H, J = 7.2 Hz) $-CH_3$; ^{13}C NMR ($CDCl_3$): δ = 164.9, 146.5, 128.4, 126.9, 124.8, 52.8, 31.2, 30.1, 19.5, 13.3. HRMS (ESI): $[M+H]^+$ calculated for $C_{13}H_{20}BN_4O_2$ 275.1674, found: 275.0565. IR: υ 3362, 3035, and 2963 cm^{-1}.

*[4-(2-Pentyl-2H-tetrazole-5-yl)phenethyl]boronic acid (**BF7e**)*

51.0 mg (59%) of white solid; m.p. 95–98°C. ^{1}H NMR ($CDCl_3$): δ = 8.05 (d, 2H, J = 7.8 Hz) –CH, 7.33 (d, 2H, J = 7.9 Hz) –CH, 4.84 (brd s, 1H) –OH, 4.63 (t, 2H, J = 7.1 Hz) $-CH_2$, 2.82 (t, 2H, J = 8.0 Hz) $-CH_2$, 2.20–2.00 (m, 2H) $-CH_2$, 1.45–1.30 (m, 4H) $-CH_2$, 1.22 (t, 2H, J = 8.1 Hz) $-CH_2$, 0.91 (t, 3H, J = 6.3 Hz) $-CH_3$; ^{13}C NMR ($CDCl_3$): δ = 165.0, 146.8, 128.4, 126.9, 124.7, 53.2, 30.1, 29.0, 28.4, 22.0, 13.8. HRMS (ESI): $[M+H]^+$ calculated for $C_{14}H_{22}BN_4O_2$ 289.1830, found: 289.2119. IR: υ 3375, 3031, and 2949 cm^{-1}.

*[4-(2-Hexyl-2H-tetrazole-5-yl)phenethyl]boronic acid (**BF7f**)*

206.3 mg (75%) of white solid; m.p. 82–86°C. ^{1}H-NMR ($CDCl_3$): δ = 8.07 (d, 2H, J = 8.2 Hz) –CH, 7.35 (d, 2H, J = 7.5 Hz) –CH, 4.64 (t, 2H, J = 7.1 Hz) $-CH_2$, 2.83 (t, 2H, J = 8.0 Hz) $-CH_2$, 2.20–2.00 (m, 2H) $-CH_2$, 1.50–1.20 (m, 8H) $-CH_2$, 1.00–0.80 (t, 3H) $-CH_3$; ^{13}C NMR ($CDCl_3$): δ = 164.9, 146.3, 128.4, 127.0, 125.2, 53.1, 31.5, 30.1, 29.3, 28.5, 26.3, 22.4, 13.9. HRMS (ESI): $[M+H]^+$ calculated for $C_{15}H_{24}BN_4O_2$ 303.1992, found: 303.2257. IR: υ 3370, 3029, and 2953 cm^{-1}.

*[4-(2-Heptyl-2H-tetrazole-5-yl)phenethyl]boronic acid (**BF7g**)*

137.5 mg (69%) of white solid; m.p. 84–85°C. ^{1}H NMR ($CDCl_3$): δ = 8.07 (d, 2H, J = 8.2 Hz) –CH, 7.35 (d, 2H, J = 8.0 Hz) –CH, 4.64 (t, 2H, J = 7.1 Hz) $-CH_2$, 4.30–4.25 (brd s, 1H) –OH, 2.83 (t, 2H, J = 7.9 Hz) $-CH_2$, 2.10–2.00 (m, 2H) $-CH_2$, 1.50–1.20 (m, 10H) $-CH_2$, 0.88 (t, 3H, J = 6.9 Hz) $-CH_3$; ^{13}C NMR ($CDCl_3$): δ = 164.9, 146.3, 128.4, 127.0, 125.2, 53.1, 31.5, 30.1, 29.3, 28.5, 26.3, 22.4, 13.9. HRMS (ESI): $[M+H]^+$ calculated for $C_{16}H_{26}BN_4O_2$ 317.2143, found: 317.2065. IR: υ 3228, and 2947 cm^{-1}.

*[4-(2-Octyl-2H-tetrazole-5-yl)phenethyl]boronic acid (**BF7h**)*

100.7 mg (50%) of white solid; m.p. 92–95°C. ^{1}H NMR (DMSO-d_6): δ = 7.92 (d, 2H, J = 8.0 Hz) –CH, 7.35 (d, 2H, J = 8.0 Hz) –CH, 6.50–6.40 (brd s, 1H) –OH, 4.68 (t, 2H, J = 6.9 Hz) $-CH_2$, 2.69 (t, 2H, J = 8.2 Hz) $-CH_2$, 2.00–1.85 (m, 2H) $-CH_2$, 1.30–1.10 (m, 10H) $-CH_2$, 0.93 (t, 3H, J = 7.8 Hz) $-CH_2$, 0.81 (t, 3H, J = 6.1 Hz) $-CH_3$; ^{13}C NMR (DMSO-d_6): δ = 164.6, 148.2, 129.0, 126.6, 124.6, 53.1, 31.5, 30.5, 29.1, 28.8, 28.6, 26.1, 22.4, 14.3. HRMS (ESI): $[M+H]^+$ calculated for $C_{17}H_{28}BN_4O_2$ 331.2300, found: 331.2291. IR: υ 3210, and 2920 cm^{-1}.

*[4-(2-Benzyl-2H-tetrazole-5-yl)phenethyl]boronic acid (**BF7i**)*

81.3 mg (60%) of white solid; m.p. 111–116°C. ^{1}H NMR (DMSO-d_6): δ = 7.92 (d, 2H, J = 8.0 Hz) –CH, 7.59 (s, 2H) –CH, 7.45–7.30 (m, 5H) –CH, 5.97 (s, 2H) $-CH_2$, 2.69 (t, 2H, J = 8.2 Hz) $-CH_2$, 0.94 (t, 3H, J = 8.4 Hz) $-CH_2$; ^{13}C NMR (DMSO-d_6): δ = 165.0, 148.4, 134.6, 129.3, 129.0, 128.7, 126.7, 124.3, 56.5, 30.5. HRMS (ESI): $[M+H]^+$ calculated for $C_{16}H_{18}BN_4O_2$ 309.1523, found: 309.1508. IR: υ 3249, 3029, and 2941 cm^{-1}.

4.1.4 | General procedure for the synthesis of 8-[4-(2-alkyl-2*H*-tetrazol-5-yl)phenethyl]tetrahydro-8*H*-8λ^4-[1,3,2]oxazaborolo[2,3-b][1,3,2]oxazaborole (**BF8a–e,g–i**)

The synthesis procedure of Caron et al. was used with some modifications. The appropriate alkyl boronic acid compound (1 equiv), a catalytic amount of Na_2SO_4, and diethanolamine (1.2 equiv) were added to ethyl acetate (2 mL) and refluxed for 10 h. Product formation was monitored by TLC using a hexane/ethyl acetate (1:1) solvent mixture. At the end of the reaction time, the mixture was cooled to room temperature, and filtered using filter paper to remove Na_2SO_4. The reaction solvent was evaporated under reduced pressure. Afterward, the mixture was crystallized from propan-2-ol-hexane by storing it at −20°C. The product was filtered and washed with propan-2-ol/hexane (1:5) to remove excess diethanolamine.[29]

*8-[4-(2-Methyl-2H-tetrazol-5-yl)phenethyl]tetrahydro-8H-8λ^4-[1,3,2]oxazaborolo[2,3-b][1,3,2]oxazaborole (**BF8a**)*

148.0 mg (54%) of white solid; m.p. 207–209°C. ^{1}H-NMR ($CDCl_3$): δ = 8.04 (d, 2H, J = 8.0 Hz) –CH, 7.40 (d, 2H, J = 7.9 Hz) –CH, 4.40 (s, 3H) $-CH_3$, 4.10–3.70 (m, 5H) $-CH_2$, NH, 3.10–2.90 (m, 2H) –CH, 2.77 (t, 2H, J = 7.8 Hz) $-CH_2$, 2.70–2.60 (m, 2H) –CH, 0.93 (t, 2H, J = 7.7 Hz) $-CH_2$; ^{13}C NMR ($CDCl_3$): δ = 149.3, 128.8, 127.0, 124.7, 63.0, 51.8, 39.6, 31.8. HRMS (ESI): $[M+H]^+$ $C_{14}H_{21}BN_5O_2$ 302.1799, found: 302.1819. IR: υ 3146, 3023, and 2897 cm^{-1}.

15214184, 0, Downloaded from https://onlinelibrary.wiley.com/doi/10.1002/ardp.202300382 by Gazi University, Wiley Online Library on [03/10/2023]. See the Terms and Conditions (https://onlinelibrary.wiley.com/terms-and-conditions) on Wiley Online Library for rules of use; OA articles are governed by the applicable Creative Commons License

*8-[4-(2-Ethyl-2H-tetrazol-5-yl)phenethyl]tetrahydro-8H-8λ^4-[1,3,2]oxazaborolo[2,3-b][1,3,2]oxazaborole (**BF8b**)*

17.6 mg (43%) of white solid; m.p. 186–190°C. ^{1}H NMR ($CDCl_3$): δ = 8.05 (d, 2H, *J* = 8.1 Hz) –CH, 7.40 (d, 2H, *J* = 8.0 Hz) –CH, 4.70 (q, 2H, *J* = 7.4 Hz) –CH_2, 4.00–3.80 (m, 5H) –CH, –NH, 3.10–2.90 (m, 2H) –CH, 2.77 (t, 2H, *J* = 7.8 Hz) –CH_2, 2.75–2.50 (m, 2H) –CH, 1.69 (t, 2H, *J* = 7.3 Hz) –CH_3, 0.93 (t, 2H, *J* = 7.8 Hz) –CH_2; ^{13}C NMR ($CDCl_3$): δ = 165.2, 149.2, 128.6, 126.9, 124.6, 63.0, 51.7, 48.5, 31.7, 14.7. HRMS (ESI): $[M+H]^+$ calculated for $C_{15}H_{23}BN_5O_2$ 316.1945, found: 316.1965. IR: υ 3137, 3011, and 2926 cm^{-1}.

*8-[4-(2-Propyl-2H-tetrazol-5-yl)phenethyl]tetrahydro-8H-8λ^4-[1,3,2]oxazaborolo[2,3-b][1,3,2]oxazaborole (**BF8c**)*

18.8 mg (57%) of white solid; m.p. 170–173°C. ^{1}H NMR ($CDCl_3$): δ = 8.04 (d, 2H, *J* = 8.1 Hz) –CH, 7.40 (d, 2H, *J* = 8.4 Hz) –CH, 4.61 (t, 2H, *J* = 7.0 Hz) –CH_2, 4.20–3.80 (m, 5H) –CH_2, –NH, 3.15-2.95 (m, 2H) –CH, 2.76 (t, 2H, *J* = 7.7 Hz) –CH_2, 2.70–2.50 (m, 2H) –CH, 2.20–2.00 (m, 2H) –CH_2, 1.00 (t, 3H, *J* = 7.4 Hz), 0.92 (t, 2H, *J* = 6.7 Hz) –CH_2; ^{13}C NMR ($CDCl_3$): δ = 165.1, 149.1, 128.4, 126.6, 124.3, 62.8, 54.6, 51.5, 31.6, 22.8, 10.9. HRMS (ESI): $[M+H]^+$ calculated for $C_{16}H_{25}BN_5O_2$ 330.2132, found: 330.2149. IR: υ 3073, 3019, and 2983 cm^{-1}.

*8-[4-(2-Butyl-2H-tetrazol-5-yl)phenethyl]tetrahydro-8H-8λ^4-[1,3,2]oxazaborolo[2,3-b][1,3,2]oxazaborole (**BF8d**)*

25.4 mg (57%) of white solid; m.p. 156–157°C. ^{1}H NMR ($CDCl_3$): δ = 8.03 (d, 2H, *J* = 8.1 Hz) –CH, 7.38 (d, 2H, *J* = 8.0 Hz) –CH, 4.64 (t, 2H, *J* = 7.0 Hz) –CH_2, 4.20–3.80 (m, 5H) –CH_2, –NH, 3.20–2.90 (m, 2H) –CH, 2.80–2.60 (m, 4H) –CH, –CH_2, 2.20–2.00 (m, 2H) –CH_2, 1.50–1.30 (m, 2H) –CH_2, 1.10–0.80 (m, 5H) –CH_2, –CH_3; ^{13}C NMR ($CDCl_3$): δ = 165.2, 149.2, 128.6, 126.9, 124.6, 63.0, 53.2, 51.7, 31.7, 31.4, 19.7, 13.4. HRMS (ESI): $[M+H]^+$ calculated for $C_{17}H_{27}BN_5O_2$ 344.2258, found: 344.2278. IR: υ 3133, 3037, and 2953 cm^{-1}.

*8-[4-(2-Pentyl-2H-tetrazol-5-yl)phenethyl]tetrahydro-8H-8λ^4-[1,3,2]oxazaborolo[2,3-b][1,3,2]oxazaborole (**BF8e**)*

21.6 mg (55%) of white solid; m.p. 146–149°C. ^{1}H NMR ($CDCl_3$): δ = 8.06 (d, 2H, *J* = 8.0 Hz) –CH, 7.40 (d, 2H, *J* = 8.0 Hz) –CH, 4.64 (t, 2H, *J* = 7.0 Hz) –CH_2, 4.10–3.80 (m, 4H) –CH, 3.70–3.60 (s, NH), 3.10–2.90 (m, 2H) –CH, 2.85–2.60 (m, 4H) –CH, –CH_2, 2.20–2.00 (m, 2H) –CH_2, 1.50–1.30 (m, 4H) –CH_2, 1.10–0.85 (m, 5H) –CH_2, –CH_3; ^{13}C NMR ($CDCl_3$): δ = 165.1, 149.2, 128.5, 126.7, 124.4, 62.8, 53.1, 51.5, 31.6, 29.0, 28.4, 21.9, 13.8. HRMS (ESI): $[M+H]^+$ calculated for $C_{18}H_{29}BN_5O_2$ 358.2414, found: 358.2436. IR: υ 3077, 3021, and 2949 cm^{-1}.

*8-[4-(2-Heptyl-2H-tetrazol-5-yl)phenethyl]tetrahydro-8H-8λ^4-[1,3,2]oxazaborolo[2,3-b][1,3,2]oxazaborole (**BF8g**)*

20.3 mg (48%) of white solid; m.p. 140–142°C. ^{1}H NMR ($CDCl_3$): δ = 8.06 (d, 2H, *J* = 8.2 Hz) –CH, 7.40 (d, 2H, *J* = 8.0 Hz) –CH, 4.65 (t, 2H, *J* = 7.2 Hz) –CH_2, 4.05–3.75 (m, 5H) –CH_2, –NH, 3.15–3.00 (m, 2H) –CH, 2.85–2.60 (m, 4H) –CH, –CH_2, 2.20–2.00 (m, 2H) –CH_2, 1.40–1.20 (m, 8H) –CH_2, 1.00–0.80 (m, 5H) –CH_2, –CH_3; ^{13}C NMR ($CDCl_3$): δ = 164.2, 148.2, 127.7, 126.0, 124.9, 62.0, 52.3, 50.8, 30.7, 30.6, 28.5, 27.7, 25.4, 21.6, 13.1. HRMS (ESI): $[M+H]^+$ calculated for $C_{20}H_{33}BN_5O_2$ 386.2727, found: 386.2755. IR: υ 3117, 3022, and 2921 cm^{-1}.

*8-[4-(2-Octyl-2H-tetrazol-5-yl)phenethyl]tetrahydro-8H-8λ^4-[1,3,2]oxazaborolo[2,3-b][1,3,2]oxazaborole (**BF8h**)*

23.0 mg (48%) of white solid; m.p. 122–125°C. ^{1}H NMR ($CDCl_3$): δ = 8.05 (d, 2H, *J* = 8.0 Hz) –CH, 7.40 (d, 2H, *J* = 7.9 Hz) –CH, 4.64 (t, 2H, *J* = 7.2 Hz) –CH_2, 4.10–3.75 (m, 5H) –CH_2, –NH, 3.15–2.95 (m, 2H) –CH, 2.85–2.60 (m, 4H) –CH, –CH_2, 2.15–2.00 (m, 2H) –CH_2, 1.45–1.20 (m, 10H) –CH_2, 1.00–0.80 (m, 5H) –CH_2, –CH_3; ^{13}C NMR ($CDCl_3$): δ = 165.0, 149.0, 128.6, 126.8, 124.7, 62.8, 53.1, 51.6, 31.6, 31.6, 29.3, 28.9, 28.8, 26.3, 22.5, 14.0. HRMS (ESI): $[M+H]^+$ calculated for $C_{21}H_{35}BN_5O_2$ 400.2884, found: 400.2907. IR: υ 3136, 3029, and 2953 cm^{-1}.

*8-[4-(2-Benzyl-2H-tetrazol-5-yl)phenethyl]tetrahydro-8H-8λ^4-[1,3,2]oxazaborolo[2,3-b][1,3,2]oxazaborole (**BF8i**)*

23.0 mg (66%) of white solid; m.p. 208–211°C. ^{1}H NMR (DMSO-d_6): δ = 7.89 (d, 2H, *J* = 8.0 Hz) –CH, 7.45–7.25 (m, 7H) –CH, 6.76 (s, 1H) –NH, 5.96 (s, 2H) –CH_2, 3.80–3.55 (m, 4H) –CH, 3.10–2.90 (m, 2H) –CH, 2.80–2.65 (m, 2H) –CH, 2.55–2.40 (m, 2H) –CH, 0.60–0.45 (m, 2H) –CH_2; ^{13}C NMR (DMSO-d_6): δ = 165.6, 151.1, 135.1, 129.8, 129.5, 129.4, 129.2, 127.0, 124.3, 63.1, 56.9, 51.6, 32.6. HRMS (ESI): $[M+H]^+$ calculated for $C_{20}H_{25}BN_5O_2$ 378.2101, found: 378.2109. IR: υ 3094, 3019, and 2878 cm^{-1}.

4.1.5 | Synthesis of 2-bromo-1-[4-(2-methyl-2*H*-tetrazole-5-yl)phenyl]ethan-1-one (**Ac2**)

The synthesis procedure of Prokopowicz et al. was followed with slight modifications. 1-[4-(2-Methyl-2*H*-tetrazol-5-yl)phenyl] ethan-1-one (0.75 g, 3.99 mmol) was dissolved in 30 mL of $CHCl_3$, to which of Br_2 (0.64 g, 3.99 mmol) in 10 mL of $CHCl_3$ was added via a dropping funnel. After addition, the reaction was allowed to stir at room temperature. The reaction was monitored using TLC with a hexane/ethyl acetate (1:1) solvent mixture. The reaction mixture was then extracted with 15 mL of water, 15 mL of saturated sodium hydrogen carbonate solution, and 2 × 10 mL of 10% $Na_2S_2O_3$ solution. The chloroform phase was dried over Na_2SO_4 and filtered. The desired product was isolated by flash chromatography using a solvent pair of hexane/ethyl acetate (1:1). The resulting white solid was crystallized with ethyl acetate-hexane.[30] 403.2 mg (36%) of white solid; ^{1}H NMR ($CDCl_3$): δ = 8.27 (d, 2H, *J* = 8.2 Hz) –CH, 8.11 (d, 2H, *J* = 8.2 Hz) –CH, 4.50 (s, 2H) –CH_2, 4.44 (s, 3H) –CH_3; ^{13}C NMR ($CDCl_3$): δ = 190.7, 164.0, 135.0, 132.2, 129.5, 127.1, 39.6, 30.7. HRMS (ESI): $[M+Na]^+$ calculated for $C_{10}H_9BrN_4NaO$ 302.9857, found: 302.9849. IR: υ 3056, 2952, and 1690 cm^{-1}.

15214184, 0, Downloaded from https://onlinelibrary.wiley.com/doi/10.1002/ardp.202300382 by Gazi University, Wiley Online Library on [03/10/2023]. See the Terms and Conditions (https://onlinelibrary.wiley.com/terms-and-conditions) on Wiley Online Library for rules of use; OA articles are governed by the applicable Creative Commons License

4.1.6 | Synthesis of diethyl 2-acetamido-2-{2-[4-(2-methyl-2*H*-tetrazol-5-yl)phenyl]-2-oxoethyl} malonate (**Ac3**)

The synthesis procedure of Zivkovic et al. was carried out with slight modifications. Diethyl acetamido malonate (0.70 g, 3.20 mmol) was slowly added to a mixture of sodium hydride (0.13 g, 5.34 mmol) in THF at 0°C. The NaH-DEAM mixture was stirred at room temperature for 1 h. 2-Bromo-1-[4-(2-methyl-2*H*-tetrazol-5-yl)phenyl]ethan-1-one (0.30 g, 1.07 mmol) was then added to the THF mixture at 0°C and stirred at room temperature for another hour. The reaction was monitored by a TLC plate and the solvent was removed under reduced pressure. The resulting viscous liquid was extracted with ice-cold distillate. The organic phase was dried with Na_2SO_4, and the extraction solvent was removed under reduced pressure. The desired product was isolated using flash chromatography with an ethyl acetate/chloroform (1:3) solvent pair.[31] 209.8 mg (47%) of white solid; ^{1}H NMR ($CDCl_3$): δ = 8.25 (d, 2H, J = 8.3 Hz) –CH, 8.09 (d, 2H, J = 8.5 Hz) –CH, 7.14 (s, 1H) –NH, 4.44 (s, 3H) –CH_3, 4.35–4.20 (m, 4H) –CH_2, 1.99 (s, 3H) –CH_3, 1.35–1.20 (m, 6H) –CH_3; ^{13}C NMR ($CDCl_3$): δ = 196.3, 169.5, 167.1, 164.1, 137.1, 132.0, 128.8, 127.0, 63.9, 62.9, 62.6, 42.3, 39.6, 22.9, 13.9, 13.9. HRMS (ESI): $[M+Na]^+$ calculated for $C_{19}H_{23}N_5NaO_6$ 440.1546, found: 440.1551. IR: υ 3343, 3029, 2986, 1733, 1677, and 1651 cm^{-1}.

4.1.7 | Synthesis of 3-amino-3-(hydroxymethyl)-1-[4-(2-methyl-2*H*-tetrazol-5-yl)phenyl]butane-1,4-diol hydrochloride (**FTYAc1**)

The synthesis procedure of Hamada et al. was performed with slight modifications. To 5 mL of ethyl alcohol, diethyl 2-acetamido-2-{2-[4-(2-methyl-2*H*-tetrazol-5-yl)phenyl]-2-oxoethyl}malonate (0.20 g, 0.48 mmol) and $NaBH_4$ (0.11 g, 2.87 mmol) were added and stirred at room temperature for 5 min. Then, water (0.60 mL) and dry $CaCl_2$ (0.16 g, 1.44 mmol) were added to the reaction and stirred at room temperature for 16 h. After 16 h, the reaction was acidified to pH 2–3 (1 M HCl) after checking with TLC using the EtOAc/MeOH (3:1) solvent pair. Extraction was carried out with EtOAc (4 × 15 mL). The ethyl acetate phases were combined, dried over Na_2SO_4, and removed by a rotary evaporator. It was used directly in the next reaction without further purification.

N-{1-Hydroxy-2-(hydroxymethyl)-4-[4-(2-methyl-2*H*-tetrazol-5-yl)phenyl]-4-oxobutan-2-yl}acetamide (0.48 mmol) and acetic anhydride (0.34 g, 4.31 mmol) were dissolved in pyridine (5 mL). The mixture was stirred at room temperature for 16 h. After 16 h, the reaction was acidified to pH 2–3 (0.5 M HCl) after checking with TLC using the methanol-ethyl acetate (1:3) solvent pair. The reaction mixture was extracted with water (15 mL) and brine (15 mL), respectively. The EtOAc phase was dried over $MgSO_4$. The extraction solvent was removed under reduced pressure. It was used directly in the next reaction without further purification.

2-Acetamido-2-{2-acetoxy-2-[4-(2-methyl-2*H*-tetrazol-5-yl)phenyl]ethyl}propane-1,3-diyl diacetate (0.48 mmol) and $LiOH.H_2O$ (0.14 g, 3.34 mmol) were directly added to a solvent mixture of water (5 mL), methanol (5 mL), and THF (5 mL), and refluxed for 5 h. After 5 h, the reaction mixture was diluted with water after checking with TLC using the methanol-ethyl acetate (1:3) solvent pair. Extraction was carried out with EtOAc (4 × 15 mL). The organic phases were combined and the organic phase was washed with water (15 mL) and saturated brine, respectively. The organic phase was dried over $MgSO_4$ and the extraction solvent was removed in a rotary evaporator under reduced pressure. It was used directly in the final reaction step without further purification.

3-Amino-3-(hydroxymethyl)-1-[4-(2-methyl-2*H*-tetrazol-5-yl)phenyl]butane-1,4-diol (0.48 mmol) was dissolved in a mixture of MeOH/EtOAc (5:5 mL), and 4 M HCl (5 mL) was added to the reaction flask. The solvents were removed in a rotary evaporator not exceeding the temperature of 50°C. The pale-yellow viscous liquid was dissolved in ethyl acetate and allowed to crystallize.[32]

37.9 mg (24%) of white solid; m.p. > 240°C. ^{1}H NMR ($CDCl_3$): δ = 8.05 (d, 2H, J = 8.1 Hz) –CH, 7.84 (s, 1H) –NH, 7.54 (d, 2H, J = 8.2 Hz) –CH, 5.95 (s, 1H) –OH″, 5.40 (s, 1H) –OH′, 5.10–4.95 (m, 1H) –CH, 4.42 (s, 3H) -CH_3, 3.75–3.50 (m, 4H) –CH_2, 2.00–1.75 (m, 2H) –CH; ^{13}C NMR ($CDCl_3$): δ = 164.5, 149.1, 126.8, 126.6, 126.0, 68.4, 62.0, 61.6, 60.9, 40.1. HRMS (ESI): $[M-H]^-$ calculated for $C_{13}H_{19}ClN_5O$ 328.1182, found: 328.1184. IR: υ 3319, 3023, and 2937 cm^{-1}.

4.2 | Biological assays

4.2.1 | Cell culture

U87-MG and HT-29 cells were cultured in Dulbecco's modified Eagle's medium-high glucose (DMEM-HG; Thermo Fisher) supplemented with fetal bovine serum (FBS, 10% v/v, Biological Industries) and penicillin-streptomycin (P/S, 1% v/v; Thermo Fisher). SaOs-2 cells were cultured in DMEM-HG supplemented with FBS (15% v/v) and P/S (1% v/v). The cells were cultured in a CO_2 incubator (Panasonic) at 37°C and 5% CO_2 conditions. The media were refreshed every 3 days until the cells reached the confluence.

4.2.2 | XTT assay

The HT-29, SaOs-2, and U87-MG cancer cells (~50,000 cells/well, 96-well plate) were cultured for 24 h to enable cell adhesion and stabilize cell metabolism. Later, boron-conjugated drugs, including BF8a, BF8b, BF8c, BF8d, BF8e, BF8g, BF8h, BF8i, BF7a, and the control drug (FTYAc1), were applied to cultured HT-29, SaOs-2, and U87-MG cells. Additionally, 5′FU, a well-known anticancer drug, was also administered to these cell lines. After drug treatment for 72 h, an XTT test (Biological Industries) was

15214184, 0, Downloaded from https://onlinelibrary.wiley.com/doi/10.1002/ardp.202300382 by Gazi University, Wiley Online Library on [03/10/2023]. See the Terms and Conditions (https://onlinelibrary.wiley.com/terms-and-conditions) on Wiley Online Library for rules of use; OA articles are governed by the applicable Creative Commons License

performed. The cells were washed and treated with XTT reagent (50 µL). Absorbance values were recorded at 490 nm with a Multiskan Sky Microplate Spectrophotometer (Thermo Fisher).

4.2.3 | Apoptosis-necrosis assay

To visualize the impacts of boron-conjugated BF8a, administered at a dose of 20 µg/mL as determined by the XTT assay, it was observed that BF8a exhibited the least reduction in cellular proliferation after 72 h and induced lower levels of apoptosis and necrosis in HT-29, SaOs-2, and U87-MG cells. The cells (100,000 cells/well) were seeded and cultured for 24 h before drug treatments. Then, BF8a drug-included mediums were exchanged for normal mediums of cells and as control cells without drug-included mediums and were cultured for 72 h. For the apoptosis-necrosis assay, the cells were washed two times with PBS, and Apopxin Green (stains green apoptotic cells) and 7-AAD (stains red necrotic cells) were applied to the cells to stain apoptotic and necrotic cells. The cytoplasm of the living cells was stained with Cytocalcein Violet 450. The cells were visualized under a fluorescent microscope at green, red, and blue channels after the samples were incubated for 30 min at room temperature.

4.2.4 | Metabolomics

Metabolomics analyses were carried out using GC-MS. Briefly, cell-seeded plates were taken out from the incubator after 72 h, and metabolites were treated with myristic acid (1 ppm) containing methanol/H_2O (9:1, v/v, 1 mL) solution. Then, samples were soaked in liquid nitrogen for 15–20 s to prevent from disintegration of metabolites and proteins. Polar metabolites in the upper phase kept for metabolomic analyses at −80°C were transferred to new Eppendorf tubes and completely dried, then they were methoxy aminated by 20 µL methoxyamine hydrochloride (20 µg/mL in pyridine) at 30°C for 90 min and derivatized by *N*-methyl-*N*-trimethylsilyl trifluoroacetamide + 1% trimethylchlorosilane (MSTFA + 1% TMCS) reagents for 30 min at 37°C. Derivatized samples were transferred to silylated vials and analyzed with GC-MS (GC-MS-QP-2010 Ultra system, Shimadzu) using a DB5-MS column (30 m + 10 m duraguard × 0.25 mm i.d. and 0.25-µm film thickness).

The deconvolution, retention time correction, and data matrix creation were performed with MS-DIAL (ver. 4.60.) for GC-MS separation, and the data matrix was normalized according to the total peak area (TIC). Any metabolite feature with more than 50% of missing values was excluded from the data matrix. The mass features were identified using the Fiehn Retention Index Library for GC-MS analysis. The data matrix was uploaded into MetaboAnalyst (ver. 5.0) for statistical analysis. PLS-DA plots were performed to reveal the discrimination between groups. VIP graphs were plotted to specify the top 15 metabolites in discrimination between groups. Pathway analyses were performed with the significant metabolites ($p < 0.05$) by MetaboAnalyst5.0.

4.2.5 | Statistics

The XTT results of boron-bound drugs were analyzed with one-way analysis of variance (ANOVA), bars represent mean ± SEM using Excel (for Windows, Microsoft Office, 2021). A heatmap of XTT results was created with GraphPad Prism 9 (for Windows, GraphPad Software, www.graphpad.com). The images of apoptosis and necrosis assay were analyzed through ImageJ software for counting of cells with different fluorescents and counted cells were graphed and analyzed by using Origin (Pro) (Version 2022, OriginLab Corporation). Metabolomics statistical results were analyzed with Fisher's LSD one-way ANOVA and pairwise comparisons of metabolomics results performed using two-sample *t* tests ($p < 0.05$) by MetaboAnalyst5.0 (https://www.metaboanalyst.ca/).

4.3 | Molecular docking

Maestro 13.5 (Maestro, Schrödinger, LLC, 2023) was used for the preparation of ligands of BF8 series, proteins, grids, and docking process. The protein preparation was performed using the crystal structure of the target protein from the Protein Data Bank (PDB No: 6OQI, 7BMG, and 3FUG).[33–35] The preparation of ligands was carried out using the OPLS4 force field LigPrep module (LigPrep, Schrödinger, LLC, 2023). Possible ionization states were generated at the target side at pH 7.0 ± 2.0. The docking grid size was adjusted to 20 Å.[36] All ligands were docked with the target protein with extra precision. For validation, the co-crystal ligands were isolated from the crystal structure of the protein, minimized, and then docked again. The RMSD values of all co-crystal ligands (4XT2, 7BMG, and 3FUG) were calculated to be 1.410, 1.066, and 0.720 Å, respectively. The interaction between the ligand and protein was visualized using Schrodinger's XP.

ACKNOWLEDGMENTS

This study constitutes Doğukan Doyduk's PhD thesis. Therefore, the authors wish to thank the Gazi University Scientific Research Projects Unit (BAP Project No: 05/2020-25) for their financial support; and also Prof. Dr. Yunus Zorlu for his association with X-ray crystallography studies.

CONFLICTS OF INTEREST STATEMENT

The authors declare no conflicts of interest.

ORCID

Doğukan Doyduk http://orcid.org/0000-0002-1260-8879
Yılmaz Yıldırır http://orcid.org/0000-0001-9091-5324

REFERENCES

[1] S. J. Baker, J. W. Tomsho, S. J. Benkovic, *Chem. Soc. Rev.* **2011**, *40*, 4279. https://doi.org/10.1039/c0cs00131g
[2] D. B. Diaz, A. K. Yudin, *Nat. Chem.* **2017**, *9*, 731. https://doi.org/10.1038/nchem.2814

15214184, 0, Downloaded from https://onlinelibrary.wiley.com/doi/10.1002/ardp.202300382 by Gazi University, Wiley Online Library on [03/10/2023]. See the Terms and Conditions (https://onlinelibrary.wiley.com/terms-and-conditions) on Wiley Online Library for rules of use; OA articles are governed by the applicable Creative Commons License

[3] F. Yang, M. Zhu, J. Zhang, H. Zhou, *MedChemComm.* **2018**, *9*, 201. https://doi.org/10.1039/c7md00552k
[4] K. Messner, B. Vuong, G. K. Tranmer, *Pharmaceuticals* **2022**, *15*, 264. https://doi.org/10.3390/ph15030264
[5] Z. J. Leśnikowski, *J. Med. Chem.* **2016**, *59*, 7738. https://doi.org/10.1021/acs.jmedchem.5b01932
[6] H. Yanagië, T. Tomita, H. Kobayashi, Y. Fujii, Y. Nonaka, Y. Saegusa, K. Hasumi, M. Eriguchi, T. Kobayashi, K. Ono, *Br. J. Cancer* **1997**, *75*, 660. https://doi.org/10.1038/bjc.1997.118
[7] J. P. M. António, R. Russo, C. P. Carvalho, P. M. S. D. Cal, P. M. P. Gois, *Chem. Soc. Rev.* **2019**, *48*, 3513. https://doi.org/10.1039/c9cs00184k
[8] A. Estrada-Bernal, K. Palanichamy, A. Ray Chaudhury, J. R. Van Brocklyn, *Neuro Oncol.* **2012**, *14*, 405. https://doi.org/10.1093/neuonc/nos005
[9] Q. Liu, L. Alinari, C. S. Chen, F. Yan, J. T. Dalton, R. Lapalombella, X. Zhang, R. Mani, T. Lin, J. C. Byrd, R. A. Baiocchi, N. Muthusamy, *Clin. Cancer Res.* **2010**, *16*, 3182. https://doi.org/10.1158/1078-0432.CCR-09-2484
[10] E. Melamed, M. W. Lee, *Front. Immunol.* **2019**, *10*, 1. https://doi.org/10.3389/fimmu.2019.02954
[11] Y. Nagahara, M. Ikekita, T. Shinomiya, *J. Immunol.* **2000**, *165*, 3250. https://doi.org/10.4049/jimmunol.165.6.3250
[12] S. N. Patmanathan, L. F. Yap, P. G. Murray, I. C. Paterson, *J. Cell Mol. Med.* **2015**, *19*, 2329. https://doi.org/10.1111/jcmm.12635
[13] G. Ç. Turgut, D. Doyduk, Y. Yıldırır, S. Yavuz, A. Akdemir, A. Dişli, A. Şen, *Bioorg. Med. Chem.* **2017**, *25*, 483. https://doi.org/10.1016/j.bmc.2016.11.015
[14] M. A. Dimopoulos, F. Schjesvold, V. Doronin, O. Vinogradova, H. Quach, X. Leleu, Y. G. Montes, K. Ramasamy, A. Pompa, M. D. Levin, C. Lee, U. H. Mellqvist, R. Fenk, H. Demarquette, H. Sati, A. Vorog, R. Labotka, J. Du, M. Darif, S. Kumar, *Blood Cancer J.* **2022**, *12*, 9. https://doi.org/10.1038/s41408-021-00593-2
[15] A. Field-Smith, G. J. Morgan, F. E. Davies, *Ther. Clin. Risk Manag.* **2006**, *2*, 271. https://doi.org/10.2147/tcrm.2006.2.3.271
[16] Y. Yildirir, D. Doyduk, *Org. Commun.* **2022**, *15*, 333. https://doi.org/10.25135/acg.oc.139.2211-2633
[17] P. Schmidt, C. Stress, D. Gillingham, *Chem. Sci.* **2015**, *6*, 3329. https://doi.org/10.1039/c5sc00921a
[18] L. Wang, C. Dai, S. K. Burroughs, S. L. Wang, B. Wang, *Chemistry* **2013**, *19*, 7587. https://doi.org/10.1002/chem.201204290
[19] J. Sun, M. T. Perfetti, W. L. Santos, *J. Org. Chem.* **2011**, *76*, 3571. https://doi.org/10.1021/jo200250y
[20] Z. Akbari, R. Taghipour Dijojin, Z. Zamani, R. Haji Hosseini, M. Arjmand, *Int. J. Reprod. Biomed.* **2021**, *19*, 741. https://doi.org/10.18502/ijrm.v19i8.9622
[21] A. A. Cluntun, M. J. Lukey, R. A. Cerione, J. W. Locasale, *Trends Cancer* **2017**, *3*, 169. https://doi.org/10.1016/j.trecan.2017.01.005
[22] H. C. Yoo, Y. C. Yu, Y. Sung, J. M. Han, *Exp. Mol. Med.* **2020**, *52*, 1496. https://doi.org/10.1038/s12276-020-00504-8
[23] Z. Zhou, B. Sun, A. Nie, D. Yu, M. Bian, *Front. Cell Dev. Biol.* **2020**, *8*, 1. https://doi.org/10.3389/fcell.2020.599765
[24] N. M. Anderson, P. Mucka, J. G. Kern, H. Feng, *Protein Cell* **2018**, *9*, 216. https://doi.org/10.1007/s13238-017-0451-1
[25] Y. Zhang, J. Wang, N. Dai, P. Han, J. Li, J. Zhao, W. Yuan, J. Zhou, F. Zhou, *BMC Cancer* **2020**, *20*, 1. https://doi.org/10.1186/s12885-020-07336-9
[26] I. Amelio, F. Cutruzzolá, A. Antonov, M. Agostini, G. Melino, *Trends Biochem. Sci.* **2014**, *39*, 191. https://doi.org/10.1016/j.tibs.2014.02.004
[27] Y. Wang, R. Guan, P. Sivaguru, X. Cong, X. Bi, *Org. Lett.* **2019**, *21*, 4035. https://doi.org/10.1021/acs.orglett.9b01217
[28] Y. Ma, B. R. P. Reddy, X. Bi, *Org. Lett.* **2019**, *21*, 9860. https://doi.org/10.1021/acs.orglett.9b03740
[29] S. Caron, J. M. Hawkins, *J. Org. Chem.* **1998**, *63*, 2054. https://doi.org/10.1021/jo972141y
[30] M. Prokopowicz, P. Młynarz, P. Kafarski, *Tetrahedron Lett.* **2009**, *50*, 7314. https://doi.org/10.1016/j.tetlet.2009.10.042
[31] A. Zivkovic, H. Stark, *Tetrahedron Lett.* **2010**, *51*, 3769. https://doi.org/10.1016/j.tetlet.2010.05.051
[32] M. Hamada, M. Nakamura, M. Kiuchi, K. Marukawa, A. Tomatsu, K. Shimano, N. Sato, K. Sugahara, M. Asayama, K. Takagi, K. Adachi, *J. Med. Chem.* **2010**, *53*, 3154. https://doi.org/10.1021/jm901776q
[33] S. M. Bronner, K. A. Merrick, J. Murray, L. Salphati, J. G. Moffat, J. Pang, C. J. Sneeringer, N. Dompe, P. Cyr, H. Purkey, G. L. Boenig, J. Li, A. Kolesnikov, R. Larouche-Gauthier, K. W. Lai, X. Shen, S. Aubert-Nicol, Y. C. Chen, J. Cheong, J. J. Crawford, M. Hafner, P. Haghshenas, A. Jakalian, J. P. Leclerc, N. K. Lim, T. O'Brien, E. G. Plise, H. Shalan, C. Sturino, J. Wai, Y. Xiao, J. Yin, L. Zhao, S. Gould, A. Olivero, T. P. Heffron, *Bioorg. Med. Chem. Lett.* **2019**, *29*, 2294. https://doi.org/10.1016/j.bmcl.2019.06.021
[34] G. Chessari, I. R. Hardcastle, J. S. Ahn, B. Anil, E. Anscombe, R. H. Bawn, L. D. Bevan, T. J. Blackburn, I. Buck, C. Cano, B. Carbain, J. Castro, B. Cons, S. J. Cully, J. A. Endicott, L. Fazal, B. T. Golding, R. J. Griffin, K. Haggerty, S. J. Harnor, K. Hearn, S. Hobson, R. S. Holvey, S. Howard, C. E. Jennings, C. N. Johnson, J. Lunec, D. C. Miller, D. R. Newell, M. E. M. Noble, J. Reeks, C. H. Revill, C. Riedinger, J. D. St. Denis, E. Tamanini, H. Thomas, N. T. Thompson, M. Vinković, S. R. Wedge, P. A. Williams, N. E. Wilsher, B. Zhang, Y. Zhao, *J. Med. Chem.* **2021**, *64*, 4071. https://doi.org/10.1021/acs.jmedchem.0c02188
[35] B. Xu, X. Jiang, J. Xiong, J. Lan, Y. Tian, L. Zhong, X. Wang, N. Xu, H. Cao, W. Zhang, H. Zhang, X. Hong, Y. Zhan, Y. Zhang, T. Hu, *J. Med. Chem.* **2020**, *63*, 5841. https://doi.org/10.1021/acs.jmedchem.0c00088
[36] R. A. Friesner, R. B. Murphy, M. P. Repasky, L. L. Frye, J. R. Greenwood, T. A. Halgren, P. C. Sanschagrin, D. T. Mainz, *J. Med. Chem.* **2006**, *49*, 6177. https://doi.org/10.1021/jm051256o
[37] T. Rupp, O. Pelouin, L. Genest, C. Legrand, G. Froget, V. Castagné, *Transl. Oncol.* **2021**, *14*, 100926. https://doi.org/10.1016/j.tranon.2020.100926

SUPPORTING INFORMATION

Additional supporting information can be found online in the Supporting Information section at the end of this article.

How to cite this article: D. Doyduk, B. Derkus, B. Sari, C. C. Eylem, E. Nemutlu, Y. Yıldırır, *Arch. Pharm.* **2023**, e2300382. https://doi.org/10.1002/ardp.202300382

15214184, 0, Downloaded from https://onlinelibrary.wiley.com/doi/10.1002/ardp.202300382 by Gazi University, Wiley Online Library on [03/10/2023]. See the Terms and Conditions (https://onlinelibrary.wiley.com/terms-and-conditions) on Wiley Online Library for rules of use; OA articles are governed by the applicable Creative Commons License